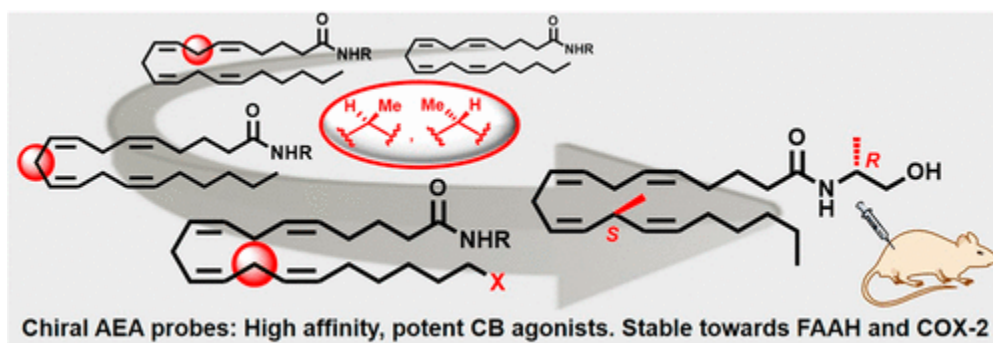# (R)-N-(1-Methyl-2-hydroxyethyl)-13-(S)-methyl-arachidonamide (AMG315): A Novel Chiral Potent Endocannabinoid Ligand with Stability to Metabolizing Enzymes

By: Yingpeng Liu, Lipin Ji, Marsha Eno, Shalley Kudalkar, Ai-Ling Li, Marion Schimpgen, Othman Benchama, Paula Morales, Shu Xu, Dow Hurst, Simiao Wu, Khadijah A. Mohammad, JodiAnne T. Wood, Nikolai Zvonok, Demetris P. Papahatjis, Han Zhou, Chandrashekhar Honrao, Ken Mackie, Patricia Reggio, Andrea G. Hohmann, Lawrence J. Marnett, Alexandros Makriyannis, and Spyros P. Nikas

Abstract:

Chiral AEA probes: High affinity, potent CB agonists. Stable towards FAAH and COX-2

The synthesis of potent metabolically stable endocannabinoids is challenging. Here we report a chiral arachidonoyl ethanolamide (AEA) analogue, namely, (13S,1′R)-dimethylanandamide (AMG315, **3a**), a high affinity ligand for the CB1 receptor (K_i of 7.8 ± 1.4 nM) that behaves as a potent CB1 agonist in vitro (EC$_{50}$ = 0.6 ± 0.2 nM). (13S,1′R)-dimethylanandamide is the first potent AEA analogue with significant stability for all endocannabinoid hydrolyzing enzymes as well as the oxidative enzymes COX-2. When tested in vivo using the CFA-induced inflammatory pain model, **3a** behaved as a more potent analgesic when compared to endogenous AEA or its hydrolytically stable analogue AM356. This novel analogue will serve as a very useful endocannabinoid probe.

Keywords: endocannabinoids | novel chiral ligand | arachidonoyl ethanolamide (AEA) analogue

Article:

Introduction

The endocannabinoids (eCBs) *N*-arachidonoylethanolamine (**1a**, AEA, Figure 1) and 2-arachidonoylglycerol (**1b**, 2-AG) are endogenously produced lipid-like substances that modulate the effects of the cannabinoid receptors CB1 and CB2, two well recognized drug targets.[1] AEA behaves as a low-efficacy agonist for CB1 and exhibits modest affinity for CB2. It has also been reported that AEA interacts with vanilloid receptors.[1] 2-AG is a high-efficacy agonist at both CB1 and CB2 and appears to be the principal endocannabinoid involved in the rapid modulation of CB1/CB2 function in CNS.[1] AEA and 2-AG are short-lived as they are hydrolytically deactivated by enzymes. Fatty acid amide hydrolase (FAAH) breaks down and inactivates AEA, while monoacylglycerol lipase (MGL) is the major enzyme responsible for 2-AG hydrolysis.[1] However, FAAH and a brain hydrolase (α/β-hydrolase domain-containing 6, ABHD6) can also inactivate 2-AG.[1,2] Additionally, the eCBs are metabolized by oxygenases including cyclooxygenases (COX-2), lipooxygenases (LOXs), and cytochrome P450 enzymes, leading to eicosanoid products with distinct, non-CB-mediated, biological actions.[3,4] COX-2 is constitutively expressed in neurons and radial glia and is upregulated in inflammatory situations where it plays a major role in eCB metabolism.[4,5] A common feature of the major oxidative metabolic pathways of the eCBs is the abstraction of a hydrogen atom from the methylene groups at C7, C10 and C13.[3]
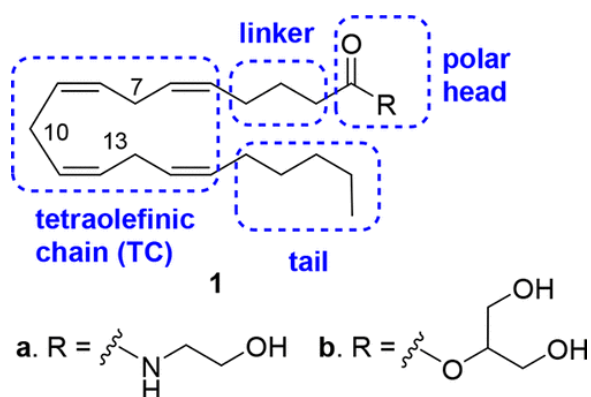

Figure 1. Structures and pharmacophoric regions of the endocannabinoids AEA (**1a**) and 2-AG (**1b**).

The four pharmacophoric regions within the structures of AEA and 2-AG (Figure 1) encompass a polar headgroup, a tetraolefinic chain (TC), an *n*-pentyl tail, and a linker which connects the headgroup with the TC.[6] Of these, the flexible TC is the major determinant of the biologically active conformation(s) of the eCBs as reflected in their binding motifs and G-protein signaling properties.[6–9] A key structural feature of the TC is the bis-allylic carbons (7, 10, and 13) that are the carbons connected to two consecutive C=C double bonds. These methylene groups can access a broad region of conformational space,[9] with the TCs exhibiting a high degree of flexibility. This situation permits the arachidonoyl moiety of the lipid to assume a number of conformations, including both folded as well as extended conformations.[9] Studies on AEA and its analogues have suggested that the folded U-, J-, or helical-shaped conformations are

responsible for CB1 receptor recognition,[7,9–11] and successful modifications at the polar head, linker, and tail groups of the AEA have been reported, with the best-known being the (*R*)-methanandamide (AM356),[9,12–16] a valuable AEA analogue which exhibits enhanced stability for FAAH. However, ethanolamides with structurally modified or constrained TCs that mimic the above types of conformations are either inactive or exhibit much lower affinities for the CB1 receptor when compared to AEA.[8,11,15,17] It is worthy of note that ethanolamides with significant affinities for CB2 have not been reported, and there are no reports on AEA analogues that are stable with the major oxidative enzyme COX-2. Recently, we reported the crystal structures of the CB1 receptor.[7,18] This breakthrough work in combination with biophysical methods,[19,20] computational studies, and currently available biochemical and in vivo assays opens the door to explore the molecular basis regarding the bioactive eCB conformation(s) as well as downstream signaling events that are associated with the in vitro and in vivo pharmacological profiles of these lipids. Taking into consideration all of the above, we report here the discovery of novel chiral AEA probes that encompass TCs with distinct conformational properties, higher binding affinities for CB1 and CB2 receptors, increased abilities to activate their molecular targets (CB1, CB2), and enhanced stabilities for their deactivating enzymes FAAH and COX-2. Our lead analogue, namely (13*S*,1′*R*)-dimethyl-anandamide (**3a**), is a novel chiral eCB ligand possessing high affinity and potency for the CB1 receptor coupled with excellent biochemical stability for FAAH, MGL, ABHD6, and COX-2. This analogue suppressed CFA-induced mechanical allodynia through a CB1 mechanism and produced greater antiallodynic efficacy than its hydrolytically stable analogue AM356.

Results and Discussion

Ligand Design. A very useful approach for the design of the novel AEA analogues with variable conformational and stability properties is the addition of chiral methyl groups in each of the three C7, C10, and C13 bis-allylic carbons of AEA (Figure 2). The value of this approach was initially recognized by our preliminary finding that addition of a methyl group at the 13*S* position of AEA led to an enhanced affinity for the CB1 receptor.[6] Our first structure–activity/–stability study in which we introduced chiral methyl groups in the bis-allylic carbons of AEA led to chiral Me-arachidonoyl ethanolamides (chiral-Me-AEAs, **2**). We showed that when methyl groups with preferred chiralities were introduced at the C7 or C13 positions, they enhanced the affinities of these analogues for CB1 and CB2 while the C10 methyl analogues were inactive. Subsequently, the most promising analogues (C13- and C7-chiral-Me-AEAs) were modified at the polar head and tail groups to further probe CB receptor recognition in tandem with increasing the stability of the amide group for FAAH. This was pursued through two design approaches. First, we preserved the recognition features of the endogenous ethanolamide head and, as in our earlier work,[15,21] we added a second chiral methyl alpha to the nitrogen atom. Second, we replaced the ethanolamine group of our lead (13*S*)-Me-AEA (**2a**) with amine groups, including bulky amines, that lack the hydroxyl group of the prototype. These design approaches led to chiral di-Me-arachidonoyl ethanolamides (chiral-di-Me-AEAs, **3**) and (13*S*)-Me-arachidonoyl amides [(13*S*)-Me-AAs, **4**].
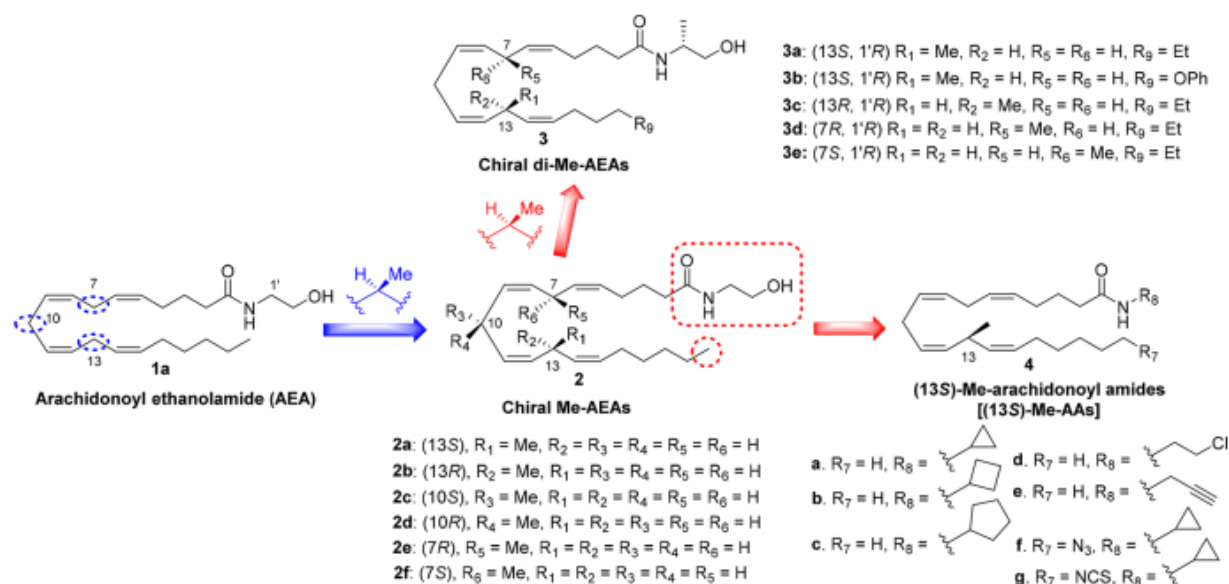
Figure 2. Design and progression of novel chiral AEA probes.

Chemistry. On the basis of our preliminary studies,[6,17,22] our optimized synthetic strategy involves key methyl ester precursors (**5**, Figure 3) from which the chiral AEA probes are produced through peptide coupling. The retrosynthetic analysis disconnects each compound at the double bonds adjacent to the chiral centers by retro-Wittig-type reactions, leading to the chiral aldehyde fragments, the headgroup fragments, and the tail fragments. The strategy was successfully executed after securing these fragments in stereochemically pure form by acetylene alkylation and selective P-2 nickel hydrogenation. Notable is the robustness of the optimized multistep enantioselective syntheses that allow the synthesis of the final compounds in substantial quantities as needed for further in vitro and in vivo studies.
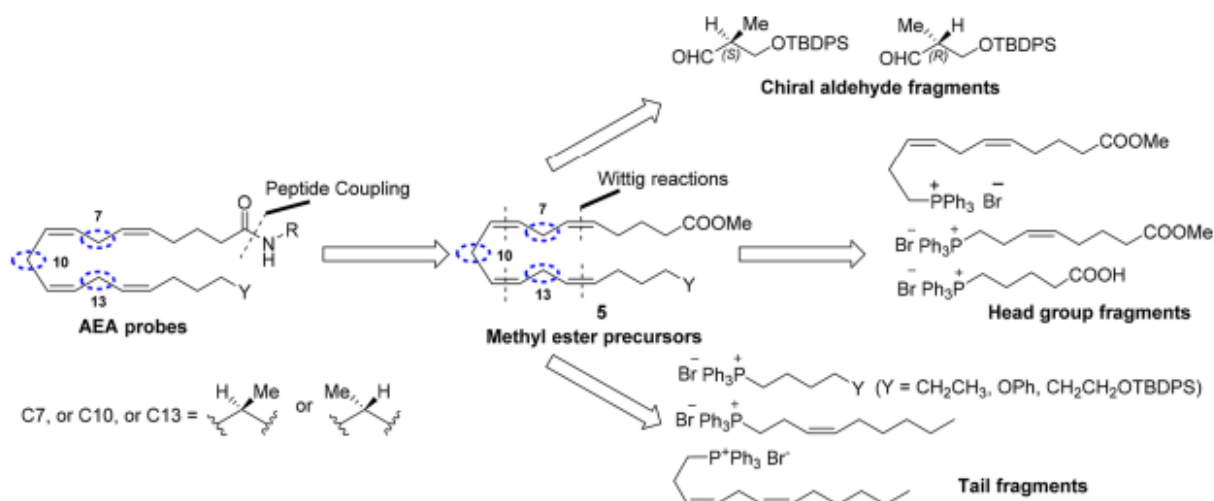

Figure 3. Retrosynthetic analysis of chiral AEA analogues.

Synthesis of the chiral aldehydes **8a** and **8b** was carried out using a modification of our earlier reported procedure[22] that improved the overall yields and reduced the synthetic steps (Scheme

1). Thus, silylation of commercially available methyl esters **6a** and **6b** gave the respective TBDPS ethers **7a** and **7b** in excellent yields (97–98%). The subsequent reduction with diisobutylaluminum hydride took place at −110 °C using 1.2 equiv of the DIBAL-H reagent and led to aldehydes **8a** and **8b** in high yields (87–88% after purification), while the formation of the overreduction byproducts alcohols was substantially suppressed (3–5%).

Scheme 1. Synthesis of the Chiral Aldehyde Fragments[a]

[a]Reagents and conditions: (a) TBDPSCl, imidazole, CH_2Cl_2, 0 °C to RT, 1.5 h, 97–98%; (b) DIBAL-H, CH_2Cl_2, −110 °C, 20 min, 87–88%.

Synthesis of the alkenyl phosphonium salt **14**, which is required for the construction of the chiral C7-Me AEA analogues, is depicted in Scheme 2. Copper mediated cross-coupling of 3-butyn-1-ol (**9**) with commercially available bromide **10** afforded diyne alcohol **11** in 93% yield. Partial hydrogenation of **11** over P-2 nickel catalyst gave the corresponding skipped *Z* diene alcohol **12** in 96% yield.[6,22] Reaction of triphenylphosphine and carbon tetrabromide with alcohol **12** under mild conditions produced bromide **13** (94% yield). Heating **13** (70–75 °C) with dry PPh$_3$ under an argon atmosphere for 5 days afforded the phosphonium salt **14** in 90% yield.[6,22] The four protons of the two double bonds in compound **14** are well separated in the ^{1}H NMR spectrum, and the coupling constants $^3J_{3H\text{-}4H}$ and $^3J_{6H\text{-}7H}$ were found to be less than 10.7 Hz. This confirms a *Z* stereochemistry between the hydrogens in the 3H–4H and 6H–7H spin systems.

Scheme 2. Synthesis of the Tail Fragment for C7-Me-AEAs[a]

[a]Reagents and conditions: (a) Cs_2CO_3, NaI, CuI, DMF, RT, 2 h, 93%; (b) Ni(OAc)$_2$, NaBH$_4$, ethylenediamine, H$_2$, MeOH, RT, 2 h, 96%; (c) CBr$_4$, Ph$_3$P, CH_2Cl_2, 0 °C, 30 min, 94%; (d) Ph$_3$P, CH$_3$CN, 70–75 °C, 5 days, 90%.

The assembly of the triphenylphosphonium bromides **14** and **15** (commercially available) with chiral aldehydes **8a** and **8b** into (7*R*)- and (7*S*)-Me-AEAs **2e** and **2f**, respectively, is outlined in Scheme 3. Thus, exposure of **15** to potassium bis(trimethylsilyl)amide at room temperature and reaction of the resulting ylide with aldehydes **8a** and **8b** at −115 °C gave the carboxylic acid derivatives **16a** and **16b**, respectively (73–75% yields). On the basis of ^{1}H NMR data, this Wittig reaction gave exclusively the *Z* alkenes with $^3J_{5H\text{-}6H} \sim 10.7$ Hz. Exposure of **16a** and **16b** to TMSCHN$_2$ in Et$_2$O/MeOH esterified the carboxylic acid group, leading to methyl esters **17a** and **17b**, respectively.[17,22] This was followed by removal of the TBDPS group using TBAF to give **18a** and **18b** in 73–75% yields for the two steps. Dess–Martin periodinane oxidation of alcohols **18a** and **18b** led to aldehydes **19a** and **19b**, respectively. Because of their labile character, these intermediates were used immediately in the subsequent Wittig olefination reaction with phosphonium salt **14** to give the respective (7*R*)- and (7*S*)-methyl

arachidonates **20a** and **20b** in very good yields (69–71%) from alcohols **18a** and **18b**. In agreement with our earlier work on similar systems as well as prostaglandin analogues, this final Wittig olefination reaction is stereoselective and installs the C8=C9 double bond with the Z stereochemistry.[6,17,22,23] Saponification of **20a** and **20b** (LiOH in THF/H$_2$O) afforded acids **21a** and **21b** (94–96% yields) that were coupled with 2-(*tert*-butyldiphenylsilyloxy)ethanamine **23** to afford the silylated amide precursors **24a** and **24b** in excellent yields (95–97%) by using the N,N'-carbonyldiimidazole-mediated amide coupling.[17,22] Deprotection of the *tert*-butyldimethylsilyl ether was carried out by using TBAF in THF and gave the enantiomeric (7R)- and (7S)-methyl anandamides **2e** and **2f**, respectively, in 85–88% yields.
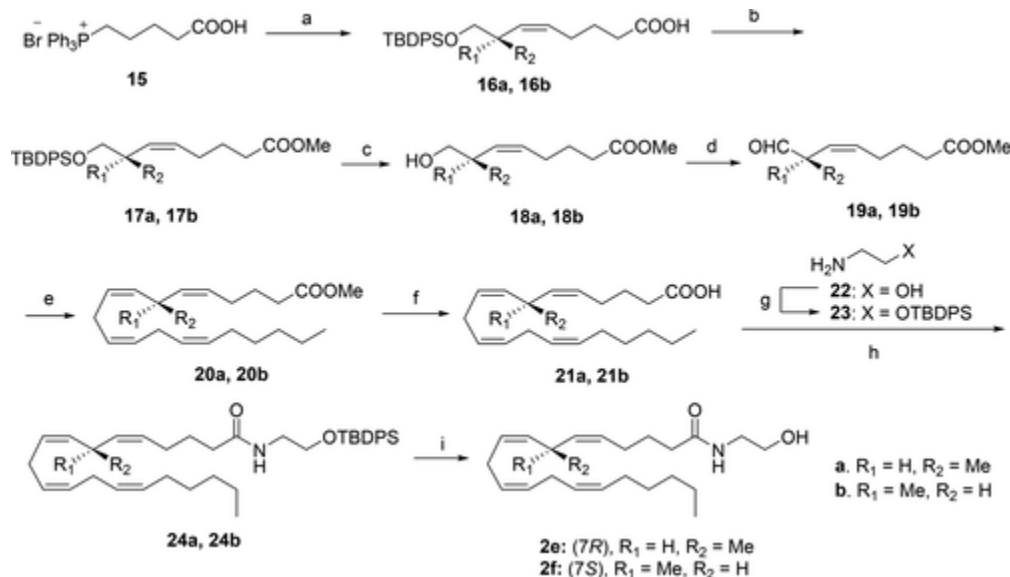
Scheme 3. Synthesis of (7R)- and (7S)-Me-AEAs[a]

[a]Reagents and conditions: (a) KHMDS, THF, RT, 1 h, then **8a**, **8b**, −115 to 0 °C, 2 h, 73–75%; (b) (trimethylsilyl)diazomethane, Et$_2$O/MeOH, RT, 30 min; (c) TBAF, THF, 0 °C to RT, 2 h, 73–75% from **16a**, **16b**; (d) Dess–Martin periodinane, CH$_2$Cl$_2$, 0 °C to RT, 1.5 h; (e) **14**, KHMDS, THF, 0 °C, 30 min, then **19a**, **19b**, −115 to −20 °C, 3 h, 69–71% from alcohols **18a**, **18b**; (f) LiOH, THF/H$_2$O, RT, 24 h, 94–96%; (g) TBDPSCl, imidazole, CH$_3$CN, 0 °C, 30 min, 97%; (h) carbonyldiimidazole, THF, RT, 2 h, then **23**, RT, 2 h, 95–97%; (i) TBAF, THF, 0 °C to RT, 1 h, 85–88%.

The enantioselective syntheses of (10S)-, (10R)-, and (13S)-methyl-anandamides **2c**, **2d**, and **2a**, respectively (Figure 2), were reported earlier from our group.[6,22] The synthesis of the (13R)-methyl-anandamide **2b** is summarized in Scheme 4 and starts from the phosphonium salt **25**. This advanced key intermediate is common for the synthesis of all (13S)- and (13R)-methyl substituted AEA analogues, and it was synthesized in multigram quantities in eight steps starting from commercially available 3-butyn-1-ol as we described earlier.[6] Wittig olefination of aldehyde **8b** with **25** at low temperature, in the presence of potassium bis(trimethylsilyl)amide, produced exclusively the desired Z-alkene product **26** in excellent yield (91%, $^3J_{11H-12H}$ = 10.8 Hz). This was followed by fluorodesilylation employing TBAF in THF and gave alcohol **27** in 91% yield. Mild oxidation of **27** with the Dess–Martin periodinane reagent led to aldehyde **28**, which was used immediately in the next step without purification. The Wittig olefination reaction of **28** with the ylide derived from hexyltriphenylphosphonium bromide and potassium bis(trimethylsilyl)amide worked well and produced methyl ester **29** in 65% yield from alcohol **27**. As expected, the Wittig reaction produced exclusively the desired Z geometrical

isomer under the experimental conditions used (low temperature, salt free). This is in full agreement with our earlier work on the (13*S*)-enantiomer (**2a**), where the *Z* stereochemistry of the C14=C15 double bond was unambiguously confirmed by using a combination of 1D and 2D NMR methods.[6] Subsequently, saponification (85% yield), CDI mediated coupling with protected ethanolamide **23** (93% yield), and fluorodesilylation with TBAF (89% yield) led to target (13*R*)-Me-AEA (**2b**).
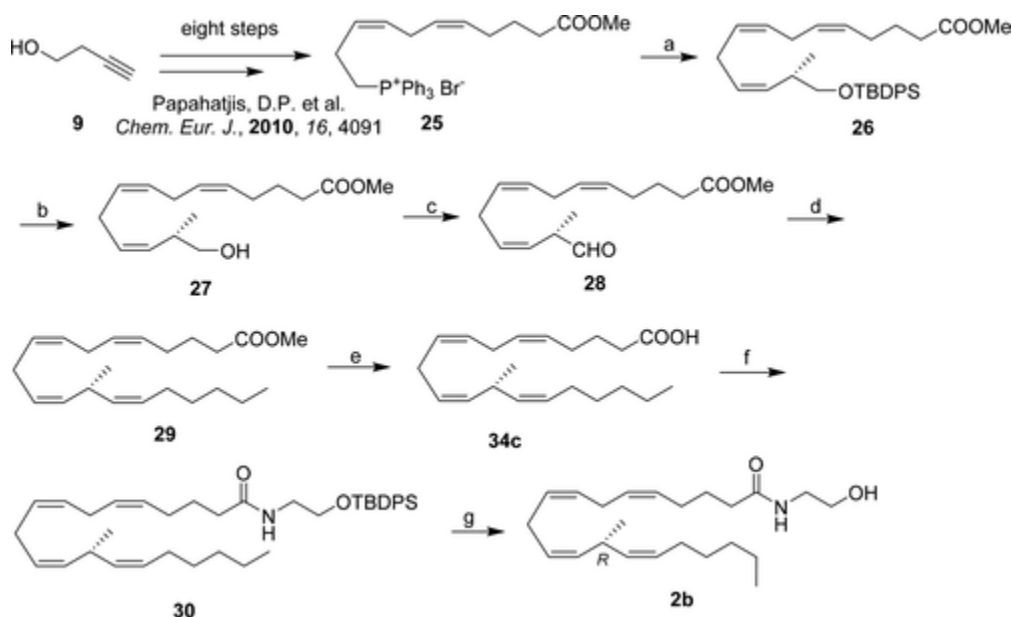

Scheme 4. Synthesis of (13*R*)-Me-AEA[a]

[a]Reagents and conditions: (a) KHMDS, THF, −78 to −60 °C, 20 min, then **8b**, −115 to 0 °C, 3 h, 91%; (b) TBAF, THF, 0 °C to RT, 1 h, 91%; (c) Dess–Martin periodinane, 0 °C to RT, 75 min; (d) CH$_3$(CH$_2$)$_5$P$^+$Ph$_3$Br$^-$, KHMDS, THF, 0 °C, 40 min, then addition of **28**, −115 to −100 °C, 50 min, 65% from alcohol **27**; (e) LiOH, THF/H$_2$O, RT, 24 h, 85%; (f) carbonyldiimidazole, THF, RT, 2 h, then **23**, RT, 1 h, 93%; (g) TBAF, THF, 0 °C to RT, 1.5 h, 89%.

The chiral di-Me-AEA analogues **3a**–**e** were synthesized in a similar manner as depicted in Scheme 5. Thus, Wittig olefination of aldehyde **8a** with **25** followed by fluorodesilylation gave the *Z* alcohol **31**.[6] The synthesis of the requisite tail modified acid **34b** was accomplished by following: (a) oxidation with Dess–Martin periodinane, (b) Wittig olefination, and (c) methyl ester hydrolysis. Eventually, amide coupling of the acids **34a**–**e** with the chiral protected ethanolamine **36** produced the intermediate silylated amides **37a**–**e** that upon treatment with TBAF afforded the chiral di-Me-AEA analogues **3a**–**e**.

Varying the head moieties of the (13*S*)-Me-substituted arachidonoyl skeleton begins with the free acid **34a** coupling to the amine derivatives to give the desired amide analogues **4a**–**e** (Scheme 6). Again, the CDI activation procedure worked well and produced these analogues in excellent yields (85–92%). Modifications at the tail aimed at incorporating azido and isothiocyanato functionalities are shown in Scheme 6. The requisite tail fragment **40** was synthesized in two steps from commercially available 6-bromo-hexan-1-ol (**38**) by using TBDPS protection and phosphonium salt formation reactions. Starting from alcohol **31** the Dess–Martin periodinane oxidation–Wittig olefination led to the intermediate methyl ester **41** in 64% overall yield. The terminal hydroxy group was then deprotected using TBAF to give **42** in 86% yield. At this point, we had established a path to synthesize the key primary alcohol **42**, which allows the

further functionalization of both the terminal tail carbon and the polar headgroup. In the current study, we focused on probes incorporating azido and isothiocyanato moieties in analogues bearing the cyclopropylamido headgroup. Thus, heating **42** with diphenylphosphoryl azide and DBU in dry DMF gave azide **43** in 71% yield. Saponification of azide ester **43** with LiOH led to acid **44** (95% yield), which was subjected to CDI-mediated amide coupling with cyclopropyl amine to give amide **4f** (74% yield). Subsequently, the isothiocyanato probe **4g** was isolated after treatment of the azido probe **4f** with carbon disulfide in the presence of triphenylphosphine (96% yield).
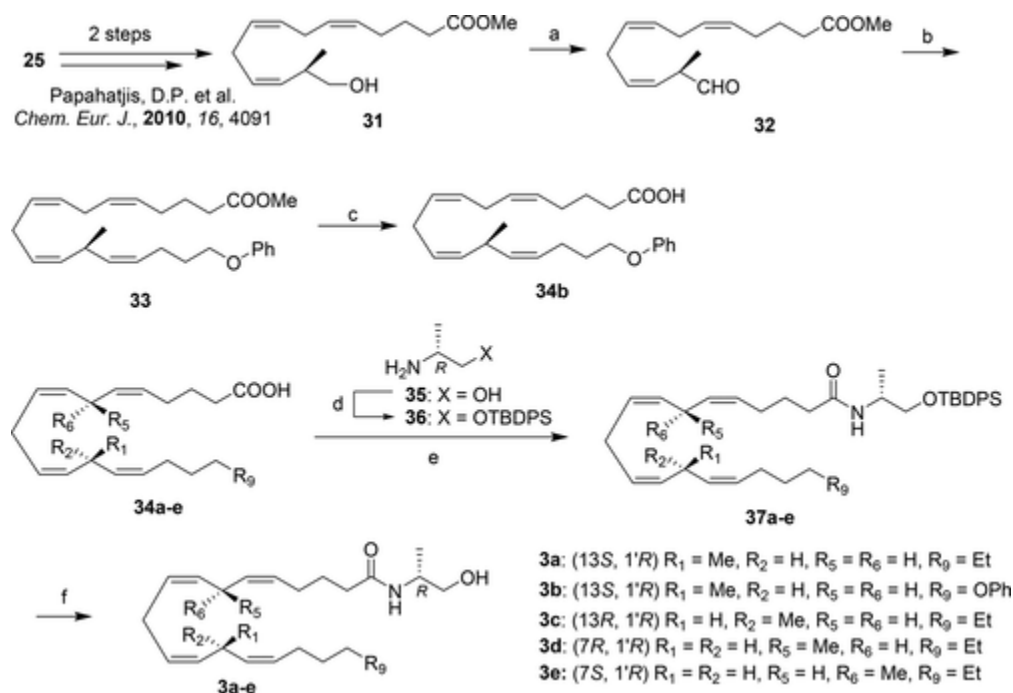
Scheme 5. Synthesis of Chiral di-Me-AEAs[a]

[a]Reagents and conditions: (a) Dess–Martin periodinane, 0 °C to RT, 3 h; (b) PhO(CH$_2$)$_4$P$^+$Ph$_3$ Br$^-$, KHMDS, THF, 0 °C, 40 min, then addition of **32**, −115 to −100 °C, 50 min, 63% from alcohol **31**; (c) LiOH, THF/H$_2$O, RT, 24 h, 87%; (d) TBDPSCl, imidazole, CH$_3$CN, 0 °C, 30 min, 95%; (e) carbonyldiimidazole, THF, RT, 2 h, then **36**, RT, 1 h, 85–92%; (f) TBAF, THF, 0 °C to RT, 1.5 h, 80–87%.

Biochemical Characterization. The synthesized chiral AEA analogues were evaluated in four steps to assess their in vitro binding affinities, functional properties, and stability for FAAH and COX-2, as follows: (1) all analogues were assessed for affinity binding to rCB1, mCB2, and hCB2; (2) the most promising compounds from each series were further evaluated in the adenylyl cyclase (cAMP) assay as a measure of their functional in vitro potency and efficacy at the CB1 receptors; (3) all analogues were evaluated preliminarily for their stability toward FAAH by comparing the K_i values from the rCB1 binding assays in the presence and absence of the FAAH inhibitor phenylmethanesulfonylfluoride (PMSF) as we have carried out in the past (detailed below).[6,24,25] This screening process served as a guide to select key AEA probes for further studies where their stabilities for expressed human and rat FAAH were assessed precisely using LC-MS/MS. (4) Representative analogues were tested for their stability toward COX-2. The discussion of the biochemical characterization follows.
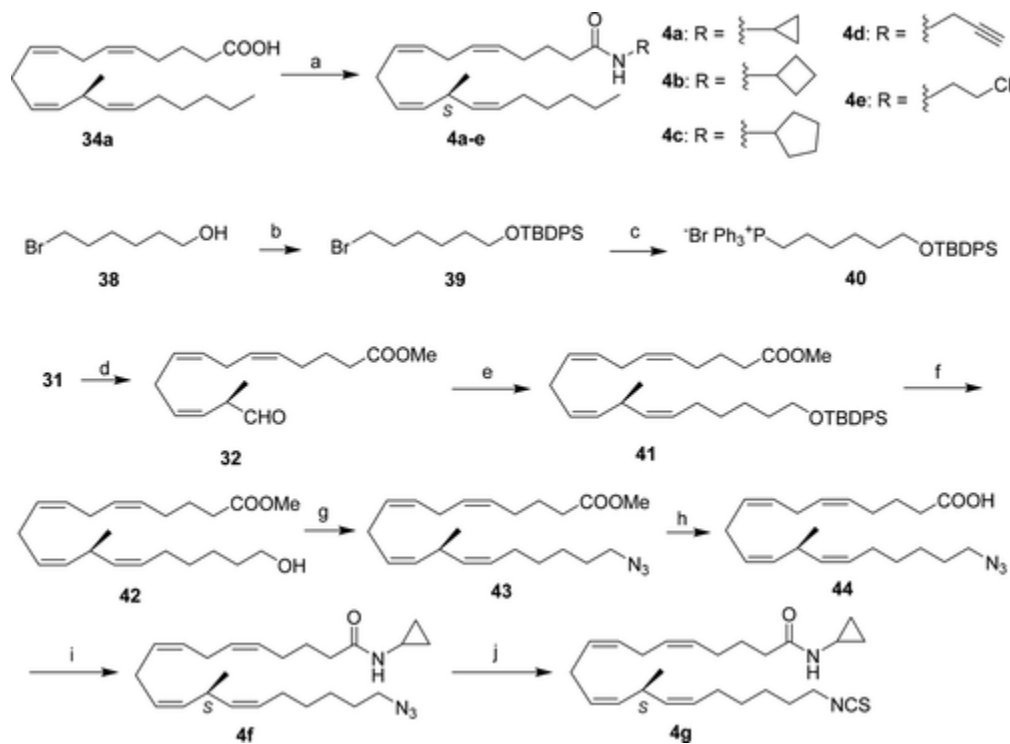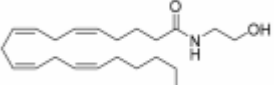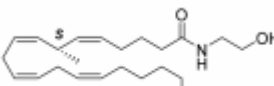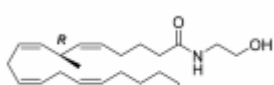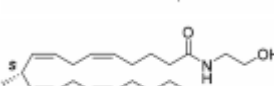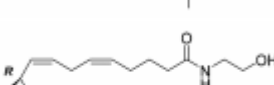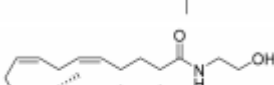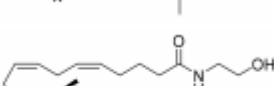
Scheme 6. Synthesis of (13*S*)-Me-arachidonoyl amides[a]

[a]Reagents and conditions: (a) carbonyldiimidazole, THF, RT, 2 h, then R-NH$_2$, RT, 1 h, 85–92%; (b) TBDPSCl, imidazole, THF, 0 °C to RT, 1.5 h, 85%; (c) Ph$_3$P, toluene, 60–63 °C, 5 days, 81%; (d) Dess–Martin periodinane, 0 °C to RT, 3 h; (e) **40**, KHMDS, THF, 0 °C, 40 min, then addition of **32**, −115 to −100 °C, 1 h, 64% from alcohol **31**; (f) TBAF, THF, 0 °C to RT, 2 h, 85%; (g) DPPA, DBU, DMF, 120 °C, 2 h, 71%; (h) LiOH, THF/H$_2$O, RT, 24 h, 95%; (i) carbonyldiimidazole, THF, RT, 2 h, then cyclopropylamine, RT, 2 h, 74%; (j) CS$_2$, PPh$_3$, THF, RT, 48 h, 96%.

a. In Vitro Biological Activity. All AEA analogues (series **2**, **3**, and **4**) were assessed for affinity binding to rCB1, mCB2, and hCB2 receptors. Competition binding experiments using [³H]CP-55,940 as the radioligand were performed in rat brain or HEK293 cell membrane preparations. As we detailed elsewhere,[6] amidase activity is present in rCB1 receptor preparations. Thus, binding experiments were carried out with and without pretreatment of the rCB1 membranes with phenylmethanesulfonyl fluoride (PMSF), a common protease inhibitor. CB2 affinity was measured by using receptor preparations where FAAH activity is absent.[6] The choice of the widely used radioligand [³H]CP-55,940 as a competing ligand for the binding assays was based on considerations discussed in our earlier publications.[6,15] Moreover, as we detailed in earlier studies, the CB2 receptor shows less homology (~82%) between species than does CB1 (~97–99%), and this may result in species-related differences in affinity. Therefore, the AEA analogues were tested on both, mouse and human CB2.[26] Functional characterization of key AEA analogues possessing the highest affinities for the rCB1 receptor was performed by measuring changes in the forskolin-stimulated cAMP as we reported earlier.[27,28]
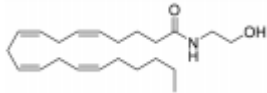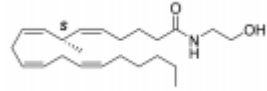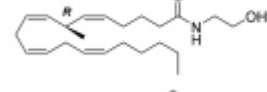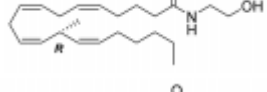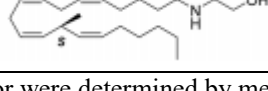
Table 1. Affinities (K_i) of Chiral-Me-AEAs (2) for CB1 and CB2 Cannabinoid Receptors (±95% Confidence Limits)

compd	Structure	(K_i, nM)[a]			
		rCBI without PMSF	rCBI with PMSF	mCB2	hCB2
AEA		>1,000	74 ± 13	>1,000	160 ± 27
AM11412 2f		>1,000	520 ± 33	>1,000	188 ± 15
AM11604 2e		326 ± 40	1.7 ± 0.1	7.5 ± 2.5	24.7 ± 5.6
AM9277 2c		>1,000	>1,000	>1,000	>1,000
AM9278 2d		>1,000	>1,000	>1,000	>1,000
AM8141 2b		>1,000	>1,000	>1,000	>1,000
AMG313 2a		>1,000	4.8 ± 1.3	137 ± 22	50.5 ± 6.5

[a] Affinities for CB1 and CB2 receptors were determined using rat brain (CB1) or membranes from HEK293 cells expressing mouse or human CB2 receptors and [^{3}H]CP-55,940 as the radioligand following previously described procedures.[6,26] Data were analyzed using nonlinear regression analysis. K_i values were obtained from three independent experiments run in duplicate and are expressed as the mean of the three values.

An examination of the binding affinity data of the chiral Me-arachidonoyl ethanolamides (chiral-Me-AEAs, **2**, Table1) shows that presence of a chiral methyl group at the tetraolefinic chain (TC) has a striking effect on the binding affinity and selectivity of the analogues for CB1 and CB2. Thus, addition of a (13S)-methyl group, compound **2a**, results in a remarkable increase in the affinity of the analogue for the CB1 receptor when compared to endogenous ligand AEA. However, the (13R)-enantiomer **2b** is inactive at both CB1 and CB2 receptors. In contrast, both the (10S) and the (10R) stereochemistry is inactive at CB1 and CB2, as seen by comparing the binding affinities of the enantiomers **2c** and **2d** (Table1). The effect of the chiral methyl group at C7 on the binding affinity of the compounds is more complex. Thus, the (7R)-enantiomer **2e** is a high affinity CB1/CB2 ligand, while the (7S)-enantiomer **2f** has low affinity for both the CB1 and CB2 receptors. Cyclase data (Table2) confirmed the effect of the stereochemistry at C7 and C13 on the bioactivity of these analogues and showed that the AEA analogues **2a** and **2e** behave as potent CB1 agonists.

Table 2. Functional Potencies (EC$_{50}$) of Novel Chiral-Me-AEAs (2) for CB1 Cannabinoid Receptor (±95% Confidence Limits)
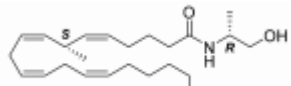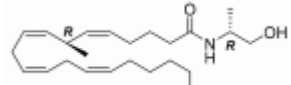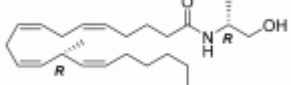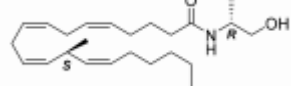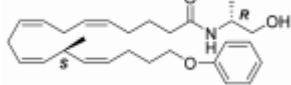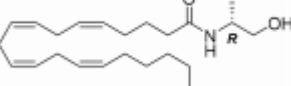
compd	Structure	rCB1 EC$_{50}$ (nM),[a] E$_{(max)}$(%)[b] classification
AEA		69 ± 10, 61% Agonist
AM11412 **2f**		No response
AM11604 **2e**		4.8 ± 1.2, 100% Agonist
AM8141 **2b**		No response
AMG313 **2a**		13.2 ± 2.8, 88% Agonist

[a] Functional potencies at rCB1 receptor were determined by measuring the decrease in forskolin-stimulated cAMP levels.[27] EC$_{50}$ values were calculated using nonlinear regression analysis. Data are the average of two independent experiments run in triplicate.
[b] Forskolin stimulated cAMP levels were normalized to 100%. E$_{(max)}$ is the maximum inhibition of forskolin stimulated cAMP levels and is presented as the percentage of CP-55,940 response at 500 nM.

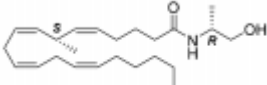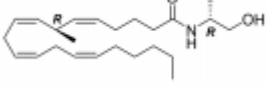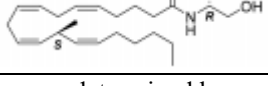Binding affinities and cyclase data for the chiral-di-Me-AEA analogues **3** are summarized in Tables 3 and 4. Our data show that addition of a second chiral methyl group at C1′ of the enantiomers **2a** and **2b** led to diastereomeric counterparts **3a** and **3c**, respectively, with similar SAR trends (Table 3). Thus, analogue **3a** with the 13*S* stereochemistry is a high affinity ligand for rCB1, while again, the 13*R* stereochemistry is not recognized by either the CB1 or the CB2 receptors (analogue **3c**). Comparisons of the binding affinities of the chiral analogues **2a** and **3a** with their achiral congeners **AEA** and **AM356**, respectively (Tables 1 and 3), confirm the superior cannabinergic activity of the chiral 13*S*-Me-AA chain versus the nonchiral AA-chain. As seen in analogue **3b**, transformation of the linear *n*-pentyl tail of the 13*S*,1′*R*-di-Me-AEA **3a** to the longer and bulkier phenoxypropyl group results in a reduction of the affinity of the analogue for the CB receptors, which is more accentuated in CB1. Incorporation of a second chiral methyl group at the C1′ of the C7-chiral-Me-AEA analogues **2e** and **2f** leads to diastereomers **3d** and **3e** (Table 3), respectively, that are both high affinity ligands for CB1 and CB2 receptors. This suggests that the C7 position is more tolerant to the structural changes when compared to C13. Our functional characterization study found that the key chiral-di-Me-AEA analogues **3a**, **3d**, and **3e** potently decrease the levels of cAMP, indicating that within this signaling mechanism these compounds behave as potent agonists at CB1 (Table 4).

Table 3. Affinities (K_i) of Chiral-di-Me-AEAs (3) for CB1 and CB2 Cannabinoid Receptors (±95% Confidence Limits)

compd	Structure	(K_i, nM)[a]			
		rCBI without PMSF	rCBI with PMSF	mCB2	hCB2
AM11414 3e		29.3 ± 3.1	21.4 ± 2.3	>1,000	120 ± 11
AM11605 3d		4.6 ± 1.3	2.2 ± 0.8	19.8 ± 4.5	12.8 ± 2.9
AMG317 3c		>1,000	>1,000	>1,000	>1,000
AMG315 3a		7.8 ± 1.4	8.9 ± 2.1	653 ± 55	176 ± 28
AMG319 3b		65 ± 9	83 ± 12	>1,000	286 ± 50
AM356		72 ± 13	37 ± 9	>1,000	220 ± 45

[a] Affinities for CB1 and CB2 receptors were determined using rat brain (CB1) or membranes from HEK293 cells expressing mouse or human CB2 receptors and [³H]CP-55,940 as the radioligand following previously described procedures.[6,26] Data were analyzed using nonlinear regression analysis. K_i values were obtained from three independent experiments run in duplicate and are expressed as the mean of the three values.
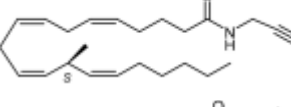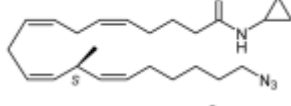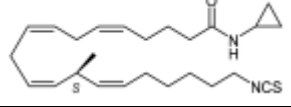
Table 4. Functional Potencies (EC_{50}) of Novel Chiral-di-Me-AEAs (3) for CB1 Cannabinoid Receptor (±95% Confidence Limits)

compd	Structure	rCB1 EC_{50} (nM),[a] $E_{(max)}$(%)[b] classification
AM11414 3e		58.3 ± 6.6, 98% Agonist
AM11605 3d		28.4 ± 4.1, 100% Agonist
AMG315 3a		0.6 ± 0.2, 76% Agonist

[a] Functional potencies at rCB1 receptor were determined by measuring the decrease in forskolin-stimulated cAMP levels.[27] EC_{50} values were calculated using nonlinear regression analysis. Data are the average of two independent experiments run in triplicate.
[b] Forskolin stimulated cAMP levels were normalized to 100%. $E_{(max)}$ is the maximum inhibition of forskolin stimulated cAMP levels and is presented as the percentage of CP-55,940 response at 500 nM.

Table 5. Affinities (K_i) of (13S)-Me-AAs (4) for CB1 and CB2 Cannabinoid Receptors (±95% Confidence Limits)

compd	Structure	(K_i, nM)[a]			
		rCBI without PMSF	rCBI with PMSF	mCB2	hCB2
AMG311 4a		14.7 ± 5.3	1.5 ± 0.3	57.5 ± 6.7	4.3 ± 1.1
AMG327 4b		17.6 ± 7.8	23.1 ± 5.1	90 ± 10	6.8 ± 0.9
AMG328 4c		123 ± 12	79 ± 8	387 ± 35	139 ± 23
AMG326 4d		8.6 ± 3.1	4.3 ± 0.6	74 ± 6	11.2 ± 3.7
AMG329 4e		45.3 ± 8.4	3.9 ± 1.4	401 ± 58	10.4 ± 2.6
AM9279 4f		10.5 ± 2.6	6.3 ± 0.7	13.3 ± 1.5	8.5 ± 1.1
AM9280 4g		20.3 ± 3.5	15.6 ± 2.1	47.7 ± 8.1	22.1 ± 3.1

[a] Affinities for CB1 and CB2 receptors were determined using rat brain (CB1) or membranes from HEK293 cells expressing mouse or human CB2 receptors and [³H]CP-55,940 as the radioligand following previously described procedures.[6,26] Data were analyzed using nonlinear regression analysis. K_i values were obtained from three independent experiments run in duplicate and are expressed as the mean of the three values.
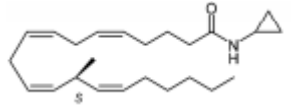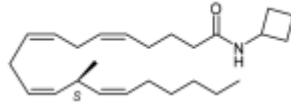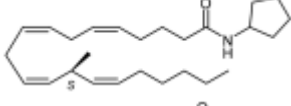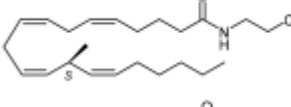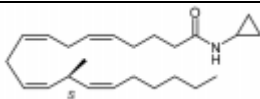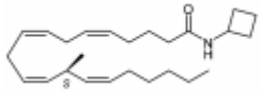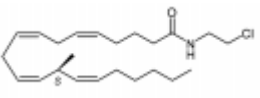
The K_i values for the (13S)-Me-arachidonoyl amides **4** are presented in Table 5 and the functional potencies of representative analogues in Table 6. We observe that the cyclopropyl (**4a**), 2′-chloroethyl (**4d**), and propargyl (**4e**) analogues have the highest binding affinities for CB1, approximately 17–70-fold higher than the endogenous AEA, while key representative analogues (**4a**, **4b**, **4d**, and **4f**) behave as potent agonists for CB1 in the cAMP assay. A cursory examination of the binding affinities of the analogues **4a**, **4b**, and **4c** for CB1 suggest that increasing the size of the cycloalkylamino headgroup from a cyclopropyl to a bulkier cyclobutyl or cyclopentyl ring leads to a progressive reduction of the affinity for CB1. Interestingly, analogues **4a**, **4b**, **4d**, and **4e** exhibit substantial binding affinity for the CB2 receptor with preference for the hCB2 versus the mCB2. To this end, the cyclobutyl analogue **4b** has a 3–13-fold preference for hCB2 over rCB1 and mCB2. Incorporation of a polar azido or isothiocyanato group at the terminal carbon atom (C20) of the chiral cyclopropylamido analogue **4a** leads to head/tail hybrid analogues **4f** and **4g** that bind equally well to both rCB1, mCB2, and hCB2 receptors. This supports a more general observation through this SAR study that combinations of the TC's chiral features with appropriate head- and/or tail-groups can generate AEA analogues with high affinity for CB2, a finding that has not been reported for AEA analogues. Additionally, analogues **4f** and **4g** carrying the photoactivatable azido and the electrophilic isothiocyanato

groups were tested for their ability to irreversibly label the rCB1 and the hCB2 receptors by following established procedures developed in our laboratory.[20,29,30] Our studies indicated that both **4f** and **4g** are not covalent binders at CB1 and CB2. Overall, our biochemical evaluation led to the discovery of novel chiral AEA ligands with distinct biological profiles including CB1 selective (e.g., **2a** and **3a**) and dual CB1/CB2 probes (e.g., **2e**, **3d**, **4a**, **4b**, **4f**, and **4g**). Key representative analogues behave as potent CB1 agonists.

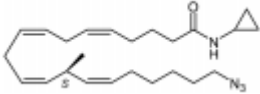**Table 6.** Functional Potencies (EC$_{50}$) of Selected (13S)-Me-AAs (4) for CB1 Cannabinoid Receptor (±95% Confidence Limits)

compd	Structure	rCB1 EC$_{50}$ (nM),[a] E$_{(max)}$(%)[b] classification
AMG311 4a		0.3 ± 0.1, 88% Agonist
AMG327 4b		36.1 ± 5.2, 92% Agonist
AMG326 4d		10.4 ± 2.6, 89% Agonist
AM9279 4f		1.9 ± 0.7, 85% Agonist

[a] Functional potencies at rCB1 receptor were determined by measuring the decrease in forskolin-stimulated cAMP levels.[27] EC$_{50}$ values were calculated using nonlinear regression analysis. Data are the average of two independent experiments run in triplicate.
[b] Forskolin stimulated cAMP levels were normalized to 100%. E$_{(max)}$ is the maximum inhibition of forskolin stimulated cAMP levels and is presented as the percentage of CP-55,940 response at 500 nM.

b. Metabolic Stability for FAAH and COX-2. Metabolic stability for AEA and representative chiral-Me-AEAs, chiral-di-Me-AEAs, and (13S)-Me-AAs are summarized in Table 7. As we reported in earlier studies, comparisons of a compound's K_i values for rCB1 obtained, with and without the presence of PMSF (see Tables 1, 3 and 5), can serve as a preliminary assessment of the stability of that compound toward FAAH hydrolysis. Thus, the rCB1 binding assays were performed twice for each AEA analogue, once after treatment of the membranes with PMSF to protect against FAAH hydrolysis, and a second time without pretreating the membranes with PMSF where enzymatic activity is not blocked.[24,25] Very little or no effect of PMSF on CB1 receptor binding affinity (K_i) is considered as an indication of enzymatic stability (see Table 7).[24,25] This preliminary screening of AEA and its analogues served as a guide to select AEA probes for further studies where their stabilities for expressed human FAAH were assessed quantitatively using LC-MS/MS methods. For species comparisons (rat versus human), AEA and one of the chiral analogues (**3d**) were tested in both rat and human FAAH preparations. Overall, our studies have identified AEA probes with excellent stability for the human FAAH enzyme including all chiral-di-Me-AEA ligands (**3**) and the (13S)-Me-AA analogues **4b**, **4c**, **4d**, **4f**, and **4g**. In addition, our data indicate that AEA is recognized equally well from both the rat and human clone, while **3d** maintains its excellent FAAH stability for both species. As in earlier work,[31] we have used a polarographic assay that measures oxygen consumption to investigate the endogenous AEA, arachidonic acid, and key analogues as substrates for mCOX-2 activity.

Data are presented in Figure 4. In agreement with our rational design, our studies indicate that incorporation of a chiral methyl group at positions C7 and C13 of the endogenous prototype enhances the stability of the TCs toward COX-2. A finding which is reported here for first time for AEA ligands. Our key analogue **3a** [(13S,1′R)-di-Me-AEA] was further tested for stability in both human MGL and human ABHD6 using HPLC methods (see Experimental Section) and found to be stable for 30 min.

Table 7. Summary of Metabolic/FAAH Stabilities of AEA and Representative Chiral-Me-AEAs (2), Chiral-di-Me-AEAs (3), and (13S)-Me-AAs (4) for FAAH

compd	rCB1 preparations without PMSF[a]	Rat (r) FAAH[b]$t_{1/2}$ (min)	Human (h) FAAH[b]$t_{1/2}$ (min)
AEA	not stable	12.1[c]	13.2[c]
2f	not stable	ND	ND
2e	not stable	ND	ND
2a	not stable	ND	13.5[c]
3a	stable	ND	stable for 30 min[c]
3e	stable	ND	ND
3d	stable	stable for 30 min[c]	stable for 30 min[c]
4a	stable	ND	25.2[c]
4b	stable	ND	stable for 30 min[c]
4d	stable	ND	stable for 30 min[c]
4c	stable	ND	stable for 30 min[c]

[a] Incubation for 1 h at 30 °C.
[b] Preparations of expressed and partially purified enzymes were used.
[c] LC-MS/MS method. ND: not determined.
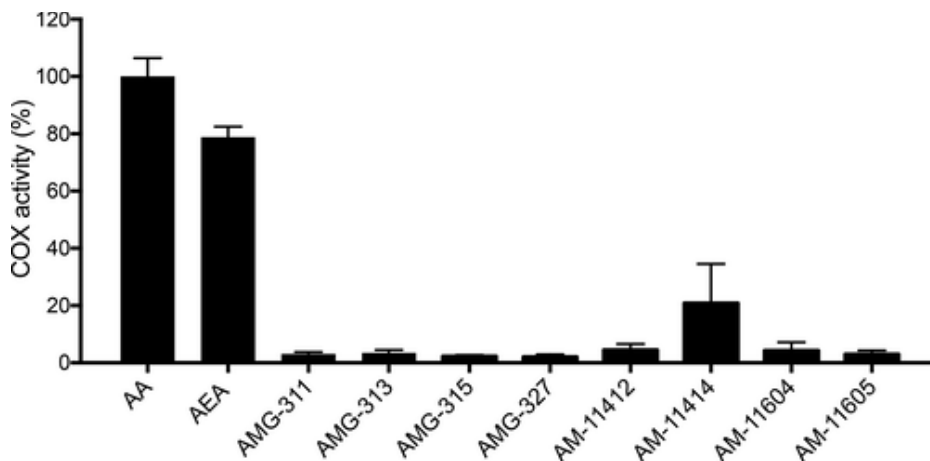
Figure 4. Oxygenation of arachidonic acid (AA), AEA, and key analogues by mCOX-2. The oxygen consumption was monitored using an oxygen electrode chamber as described in the Experimental Section.

Molecular Modeling. In an effort to understand the large binding affinity difference between the two AEA analogues, **3a** and **3c**, we performed docking studies in the CB$_1$R* model as we reported in earlier work.[20] Methods are detailed under Supporting Information. As illustrated in Figure 5A, our docking studies suggest that **3a** sits high in the receptor in the TMH2–3–6–7 region and establishes its primary interaction with K3.28. The (13S)-methyl group of **3a** defines its particular binding affinity and makes it enantioselective at CB$_1$. This stereocenter adds

conformational restriction in this region of the molecule, directing the methyl group into a hydrophobic pocket defined by K3.28, L3.29, and above V3.32, establishing strong van der Waals interactions. The alkyl tail is directed upward in the binding site, establishing hydrophobic interactions with T3.33 and Y5.39. Attempts were made to dock **3c** in the same binding pocket region as the **3a** binding site. However, the (13*R*)-methyl group of **3c** forces the ligand toward TMH6, where it has steric overlap with L6.51 (Figure 5B). This overlap precludes **3c** binding at CB1. Our docking studies provide a rational structural basis of the CB$_1$ enantioselectivity of **3a** over **3c**. Although the enantioselective actions of THC and related exogenous cannabinoids on CB1 receptor are well established, this phenomenon is observed here for first time with the endocannabinoid scaffold.
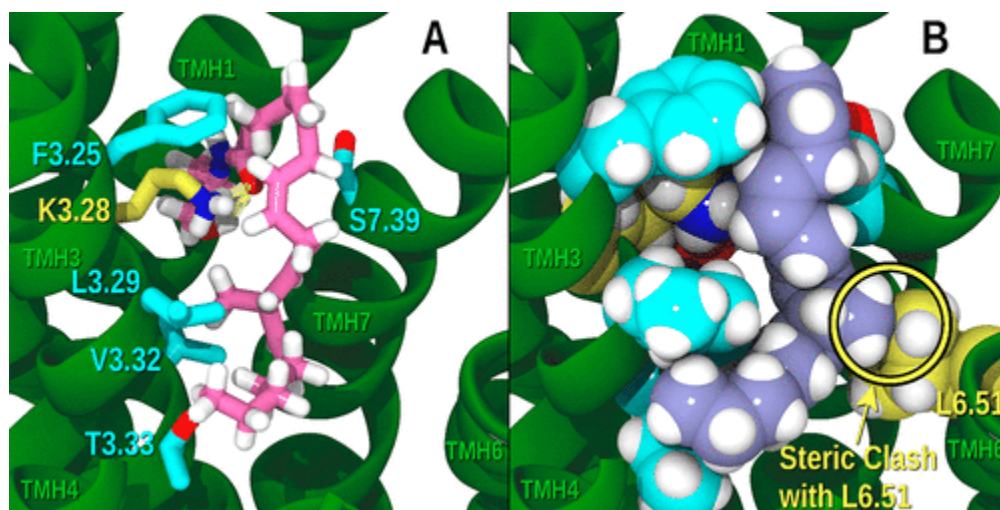
Figure 5. (A) Dock of **3a** at CB1. (B) **3c** has steric overlaps at CB1. PDB coordinates are available for 3a and 3c in the Supporting Information.

In Vivo Behavioral Characterization. *i. Results.* AMG315 produced an antiallodynic effect in CFA-induced inflammatory pain which was CB1 receptor dependent. We first examined the antiallodynic efficacy of AEA (20 mg/kg ip) in CFA-induced inflammatory pain. Intraplantar injection of CFA significantly reduced the mechanical paw withdrawal threshold on the ipsilateral side (injected paw) ($F_{1,10} = 268.2$, $p < 0.001$) to similar extent in both groups ($F_{1,10} = 0.120$, $p = 0.736$) before pharmacological treatments (Figure 6A), no group differences in inflammatory nociception was observed prior to pharmacological manipulations ($F_{1,10} = 0.016$, $p = 0.903$). During the maintenance phase of CFA-induced inflammatory pain, mechanical thresholds changed over time ($F_{3,30} = 7.161$, $p < 0.001$) but did not differ between groups ($F_{1,10} = 1.717$, $p = 0.219$), although the interaction ($F_{3,30} = 3.563$, $p = 0.026$) between groups and time were significant (Figure 6A). Bonferroni post hoc tests revealed that AEA produced only a transient antiallodynic effect at 10 min post injection ($p = 0.014$), and antiallodynic efficacy was no longer present at 30 min post injection (Figure 6A). This transient antiallodynic effect of AEA is consistent with rapid degradation of this fatty acid amide by fatty acid amide hydrolase (FAAH).
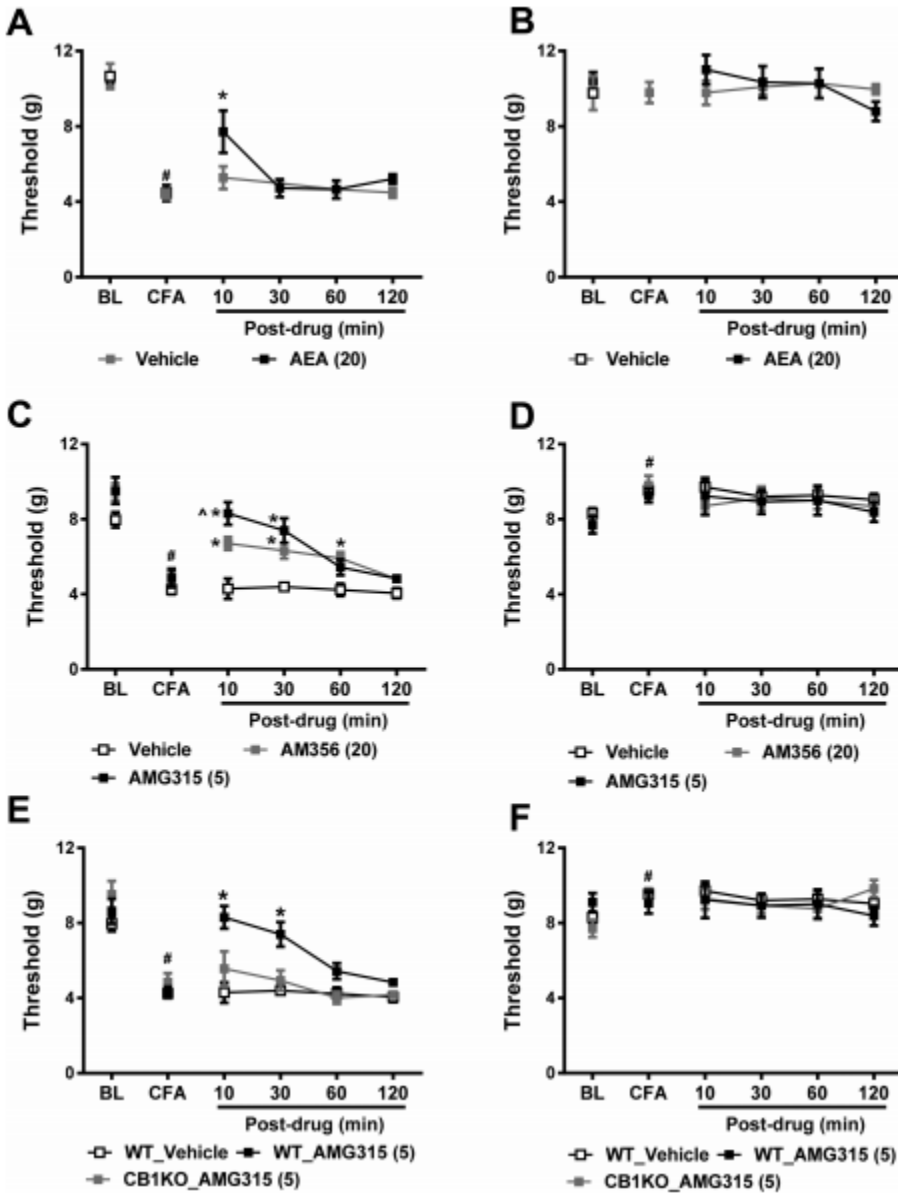
Figure 6. AMG315 reduced CFA-induced mechanical allodynia. (A) AEA (20 mg/kg ip) transiently increased the CFA-reduced mechanical paw withdrawal threshold at 10 min post injection only. (C) Both AMG315 (5 mg/kg ip) and AM356 (20 mg/kg ip) suppressed CFA-induced mechanical allodynia. Antiallodynic efficacy of AMG315 (5 mg/kg ip) was greater than that of AM356 at 10 min post injection. Antiallodynic effects were absent at 120 min post injection. (E) AMG315 (5 mg/kg ip) increase mechanical paw withdrawal thresholds in the CFA-injected paw of WT but not CB1 KO mice. (B,D,F) Pharmacological manipulations did not change the mechanical paw withdrawal threshold on the contralateral side. $*p < 0.05$ vs vehicle group; $\wedge p < 0.05$ vs AM356; $\#p < 0.05$ vs baseline. BL: baseline.

We then compared the antiallodynic effects of compounds likely to exhibit improved metabolic stability compared to AEA. We compared the antiallodynic efficacy of AMG315 (5 mg/kg ip) and AM356 (20 mg/kg ip) in the same pain model (Figure 6C). During the maintenance phase of

CFA-induced inflammatory pain, AMG315 (5 mg/kg, ip) and AM356 (20 mg/kg, ip) increased mechanical paw withdrawal thresholds ($F_{2,15} = 20.82$, $p < 0.001$) in a treatment-dependent manner ($F_{6,45} = 4.706$, $p = 0.001$) and the mechanical paw withdrawal threshold changed over time ($F_{3,45} = 16.1$, $p < 0.001$) (Figure 6C). Bonferroni post hoc tests revealed that both AMG315 (5 mg/kg) and AM356 (20 mg/kg) significantly increased mechanical paw withdrawal threshold at 10 min post injection compared with the vehicle group ($p < 0.001$) (Figure 6C). Moreover, mechanical paw withdrawal threshold was higher in CFA-injected mice that received AMG315 (5 mg/kg ip) compared to AM356 (20 mg/kg) at 10 min post injection ($p = 0.021$), consistent with improved efficacy of AMG315 compared to AM356. In contrast to AEA, both AMG315 and AM356 displayed longer duration of action which lasted up to 30 min (Figure 6C). In addition, only AM356 (20 mg/kg) increased mechanical paw withdrawal thresholds in the CFA-injected paw compared to mice receiving vehicle at 60 min post injection ($p = 0.014$). Mechanical paw withdrawal threshold in the CFA-injected paw were similar in mice receiving AMG315 and AM356 at this time point ($p = 1$).

To determine if antiallodynic effects of AMG315 were mediated by CB1 receptors, the antiallodynic effect of AMG315 (5 mg/kg, ip) was compared in WT and CB1 KO mice (Figure 6E). Postinjection mechanical paw withdrawal thresholds differed between groups and across postinjections times and the interaction between group and time was significant ($F_{2,15} = 17.545$, $p < 0.001$ [group]; $F_{3,45} = 9.67$, $p < 0.001$ [time]; $F_{6,45} = 2.961$, $p = 0.016$ [interaction]) (Figure 6E). WT mice receiving AMG315 showed elevated mechanical paw withdrawal thresholds compared to the vehicle group at 10 and 30 min post injection ($p < 0.001$). By contrast, mechanical paw withdrawal thresholds in CB1 KO mice receiving AMG315 did not differ from that of the vehicle group at any time points tested (Figure 6E). The CFA injection induced a slight increase in the mechanical paw withdrawal threshold on the contralateral side (uninjected paw), an expected consequence of uneven weight bearing of the hind paws after CFA injection (Figure 6D,F). However, pharmacological manipulations did not alter the mechanical paw withdrawal threshold of the contralateral paw during the maintenance phase of CFA-induced inflammatory pain at any time point (Figure 6B: $F_{3,30} = 1.016$, $p = 0.400$ [time]; $F_{1,10} = 0.024$, $p = 0.880$ [group]; $F_{3,30} = 1.134$, $p = 0.351$ [interaction]; Figure 6D: $F_{3,45} = 0.515$, $p = 0.674$ [time]; $F_{2,15} = 0.616$, $p = 0.553$ [group]; $F_{6,45} = 0.189$, $p = 0.978$ [interaction]; Figure 6F: $F_{3,45} = 0.328$, $p = 0.850$ [time]; $F_{2,15} = 0.835$, $p = 0.453$ [group]; $F_{6,45} = 0.499$, $p = 0.806$ [interaction]).

ii. Discussion. The metabolically stable anandamide analogue AMG315 (5 mg/kg ip) suppressed CFA-induced mechanical allodynia through a CB1 mechanism. Antinociceptive effects of AMG315 were restricted to the CFA-injected (ipsilateral) paw and were absent in the noninjected (contralateral) paw. The duration of action of AMG315 and AM356 outlasted that of AEA. AMG315 also produced greater antiallodynic efficacy than AM356 at 10 min post injection but did not exhibit a longer duration of action than AM356, suggesting possible superiority of AMG315 relative to AM356. By sparing metabolic degradation by both FAAH and COX-2, the magnitude of antiallodynic efficacy may be increased preferentially (as opposed to duration of action). The antiallodynic efficacy of AMG315 observed in WT mice was largely absent in CB1 KO mice, suggesting a CB1 mechanism of action. The same vehicle alone did not alter the responding in CB1 KO mice in our previous work.[32]

Conclusions

We report the first AEA probe, namely (13*S*,1′*R*)-dimethyl-anandamide [(13*S*,1′*R*)-di-Me-AEA, **3a**], possessing high affinity and potency for the cannabinoid CB1 receptor coupled with excellent biochemical stability for FAAH, MGL, ABHD6, and COX-2. When tested in vivo using the CFA-induced inflammatory pain model, **3a** behaved as a more potent analgesic when compared to endogenous AEA or its hydrolytically stable analogue AM356.

This was the result of a careful SAR study that led to novel AEA ligands with modified tetraolefinic chains and unique pharmacological profiles including CB1 selective (e.g., **2a** and **3a**) and dual CB1/CB2 probes (e.g., **2e**, **3d**, **4a**, **4b**, **4f**, and **4g**). Our approach for developing the novel metabolically stable AEA analogues was based on introducing chirality with conformational restriction in the tetraolefinic chain of the prototype. Key representative analogues behave as potent CB1 agonists and have enhanced stability for COX-2, while the headgroup analogues are endowed with stability toward FAAH. Unlike AEA, the chiral ligands reported here do not generate arachidonic acid which exhibits non-CB-mediated biological actions as well as in vitro and in vivo toxicity. As such, these ligands will be valuable experimental tools currently lacking for future in vitro, in vivo, and theoretical studies aimed at exploring the (patho)physiological roles of the endocannabinoid system.

Experimental Section

Materials. All reagents and solvents were purchased from Aldrich Chemical Co., unless otherwise specified, and used without further purification. All anhydrous reactions were performed under a static argon or nitrogen atmosphere in flame-dried glassware using scrupulously dry solvents. Flash column chromatography employed silica gel 60 (230–400 mesh). All compounds were demonstrated to be homogeneous by analytical TLC on precoated silica gel TLC plates (Merck, 60 F$_{245}$ on glass, layer thickness 250 μm), and chromatograms were visualized by phosphomolybdic acid staining. Melting points were determined on a micromelting point apparatus and are uncorrected. NMR spectra were recorded in CDCl$_3$, unless otherwise stated, on Varian 600 (^{1}H at 600 MHz, ^{13}C at 150 MHz), Varian 500 (^{1}H at 500 MHz), Varian 300 (^{13}C at 75 MHz), and Bruker 400 (^{1}H at 400 MHz, ^{13}C at 100 MHz) NMR spectrometers, and chemical shifts are reported in units of δ relative to internal TMS. Multiplicities are indicated as br (broadened), s (singlet), d (doublet), t (triplet), q (quartet), and m (multiplet), and coupling constants (*J*) are reported in hertz (Hz). Low and high-resolution mass spectra were performed in School of Chemical Sciences, University of Illinois at Urbana–Champaign. Mass spectral data are reported in the form of *m/z* (intensity relative to base = 100). Purities of the tested compounds were determined by LC/MS analysis using a Waters MicroMass ZQ system (electrospray ionization (ESI) with Waters-2525 binary gradient module coupled to a photodiode array detector (Waters-2996) and ELS detector (Waters-2424) using a XTerra MS C18 (5 μm, 4.6 mm × 50 mm column and acetonitrile/water) and were >95%.

*(13R,5Z,8Z,11Z,14Z)-N-(2-Hydroxyethyl)-13-methyleicosa-5,8,11,14-tetraenamide **(2b)**.* To a solution of **30** (25 mg, 0.04 mmol) in dry THF (0.8 mL) at 0 °C, under an argon atmosphere, was added tetra-*n*-butylammonium fluoride (TBAF, 0.05 mL, 0.05 mmol, 1 M solution in THF) dropwise. The reaction mixture was stirred for 10 min at 0 °C and for 1.5 h at room temperature,

and then it was quenched with saturated aqueous NH$_4$Cl at 0 °C and extracted with EtOAc. The combined organic extracts were washed with brine and dried over MgSO$_4$, and the solvent was evaporated under reduced pressure at 35–37 °C. The residue was purified by flash column chromatography on silica gel (40% EtOAc/hexane) to give **2b** (13 mg, 89% yield) as a colorless oil. ^{1}H NMR (500 MHz, CDCl$_3$) δ 0.89 (t, J = 6.9 Hz, 3H, 20-H), 1.02 (d, J = 7.2 Hz, 3H, >CH-CH_3), 1.24–1.33 (m, 4H, 18-H, 19-H), 1.35 (sextet, J = 7.2 Hz, 2H, 17-H), 1.73 (quintet, J = 7.2 Hz, 2H, 3-H), 2.06 (nonet, J = 6.3 Hz, 2H, 16-H), 2.12 (dt, J = 7.2 Hz, J = 7.2 Hz, 2H, 4-H), 2.22 (t, J = 7.6 Hz, 2H, 2-H), 2.52 (br s, 1H, −OH), 2.76–2.84 (ddd and t, overlapping, 3H, 10-H and 7-H, especially 2.81, t, J = 6.0 Hz, 2H, 7-H), 2.87 (ddd, J = 15.0 Hz, J = 7.5 Hz, J = 6.3 Hz, 1H, 10-H), 3.42 (dt, J = 5.2 Hz, J = 5.2 Hz, 2H, −CH$_2$-N<), 3.46 (sextet, J = 7.5 Hz, 1H, 13-H), 3.73 (t, J = 5.2 Hz, 2H, −CH$_2$O−), 5.20–5.31 (m, 4H, 11-H, 12-H, 14-H, 15-H), 5.44–5.32 (m, 4H, 5-H, 6-H, 8-H, 9-H), 5.88 (br s, 1H, >NH). ^{13}C NMR (150 MHz, CDCl$_3$) δ 174.16 (>C=O), 135.10 (C-12), 134.12 (C-14), 129.02 (C-8), 128.84 (C-5), 128.43 (C-6), 128.26 (C-15), 128.10 (C-9), 125.61 (C-11), 62.70 (−CH$_2$-OH), 42.48 (NH-CH$_2$), 35.92 (C-2), 31.57 (C-18), 30.50 (C-13), 29.46 (C-17), 27.51 (C-16), 26.61 (C-4), 25.84 (C-10), 25.61 (C-7), 25.44 (C-3), 22.59 (C-19), 22.04 (C-13-CH_3), 14.09 (C-20). Mass spectrum (ESI) m/z (relative intensity) 384 (M$^+$ + Na), 362 (M$^+$ + H, 100), 301 (7). Exact mass (ESI) calculated for C$_{23}$H$_{40}$NO$_2$ (M$^+$ + H) 362.3059, found 362.3047. LC/MS analysis (Waters MicroMass ZQ system) showed purity 98% and retention time 5.8 min for the title compound.

(7R,5Z,8Z,11Z,14Z)-N-(2-Hydroxyethyl)-7-methyleicosa-5,8,11,14-tetraenamide **(2e).** The synthesis was carried out as described for **2b** below, using **24a** (30 mg, 0.05 mmol) and TBAF (0.07 mL, 1 M solution in THF) in dry THF (3 mL). The reaction was completed in 1 h, and the crude oil obtained after work up was purified by flash column chromatography on silica gel (15% EtOAc/hexane) to give **2e** (15 mg, 85% yield) as a colorless oil. IR (neat): 3303, 3012, 2927, 2857, 1646 (C=O), 1543, 1275, 1261, 1066 cm^{-1}. ^{1}H NMR (500 MHz, CDCl$_3$) δ 0.89 (t, J = 6.8 Hz, 3H, 20-H), 1.02 (d, J = 6.8 Hz, 3H, >CH–CH_3), 1.23–1.41 (m, 6H, 17-H, 18-H, 19-H), 1.73 (quintet, J = 7.5 Hz, 2H, 3-H), 2.06 (dt, J = 7.3 Hz, J = 7.3 Hz, 2H, 16-H), 2.09–2.18 (m, 2H, 4-H), 2.21 (t, J = 7.5 Hz, 2H, 2-H), 2.73–2.94 (m, 4H, 10-H, 13-H), 3.38–3.50 (sextet and dt overlapping, 3H, 7-H, −CH_2-NH−), 3.72 (t, J = 5.0 Hz, 2H, −CH$_2$OH), 5.20–5.46 (m, 8H, 5-H, 6-H, 8-H, 9-H, 11-H, 12-H, 14-H, 15-H), 5.87 (br s, 1H, −NH−). ^{13}C NMR (100 MHz, CDCl$_3$) δ 174.1 (C=O), 135.3 (C=C), 134.7 (C=C), 130.5 (C=C), 128.6 (C=C), 128.0 (C=C), 127.5 (C=C), 126.8 (C=C), 125.9 (C=C), 62.7 (CH$_2$OH), 42.5 (−NHCH$_2$−), 36.0, 31.5, 30.5, 29.3, 27.2, 26.9, 25.8, 25.6, 25.5, 22.5, 22.0, 14.0. Mass spectrum (ESI) m/z (relative intensity) 362 (M$^+$ + H, 100). Exact mass (ESI) calculated for C$_{23}$H$_{40}$NO$_2$ (M$^+$ + H) 362.3059, found 362.3073. LC/MS analysis (Waters MicroMass ZQ system) showed purity 99% and retention time 5.4 min for the title compound.

(7S,5Z,8Z,11Z,14Z)-N-(2-Hydroxyethyl)-7-methyleicosa-5,8,11,14-tetraenamide **(2f).** The synthesis was carried out as described for **2b** below, using **24b** (30 mg, 0.05 mmol) and TBAF (0.07 mL, 1 M solution in THF) in dry THF (3 mL). The reaction was completed in 1 h, and the crude oil obtained after work up was purified by flash column chromatography on silica gel (15% EtOAc/hexane) to give **2f** (16 mg, 88% yield) as a colorless oil. The IR, ^{1}H NMR (500 MHz, CDCl$_3$), and ^{13}C NMR (100 MHz, CDCl$_3$) spectrum was identical to that of the enantiomer **2e**. Mass spectrum (ESI) m/z (relative intensity) 384 (M$^+$ + Na, 18), 362 (M$^+$ + H, 100), 301 (7). Exact mass (ESI) calculated for C$_{23}$H$_{40}$NO$_2$ (M$^+$ + H) 362.3059, found 362.3062.

LC/MS analysis (Waters MicroMass ZQ system) showed purity 99% and retention time 5.4 min for the title compound.

(13S,5Z,8Z,11Z,14Z)-N-((R)-1-Hydroxypropan-2-yl)-13-methyleicosa-5,8,11,14-tetraenamide (3a). To a solution of **37a** (25 mg, 0.04 mmol) in dry THF (0.8 mL) at 0 °C under an argon atmosphere was added TBAF (0.05 mL, 1 M solution in THF) dropwise. The reaction mixture was stirred for 10 min at 0 °C and for 1.5 h at room temperature, and then it was quenched with saturated aqueous NH_4Cl at 0 °C and extracted with EtOAc. The combined organic extracts were washed with brine and dried over $MgSO_4$, and the solvent was evaporated under reduced pressure at 35–37 °C. The residue was purified by flash column chromatography on silica gel (40% EtOAc/hexane) to give **3a** (13 mg, 87% yield) as a colorless oil. IR (neat): 3300, 3019, 2926, 2861, 1644 (C=O), 1540, 1273, 1262, 1069 cm^{-1}. ^{1}H NMR (600 MHz, CDCl$_3$) δ 0.89 (t, J = 6.7 Hz, 3H, 20-H), 1.02 (d, J = 6.6 Hz, 3H, =CH-CH(CH_3)−), 1.17 (d, J = 6.6 Hz, 3H, >N-CH(CH_3)−), 1.24–1.32 (m, 4H, 18-H, 19-H), 1.35 (sextet, J = 7.2 Hz, 2H, 17-H), 1.72 (quintet, J = 7.2 Hz, 2H, 3-H), 2.06 (nonet, J = 6.2 Hz, 2H, 16-H), 2.12 (dt, J = 7.2 Hz, J = 7.2 Hz, 2H, 4-H), 2.20 (t, J = 7.8 Hz, 2H, 2-H), 2.76–2.84 (ddd and t, overlapping, 3H, 10-H and 7-H, especially 2.81, t, J = 6.0 Hz, 2H, 7-H), 2.87 (ddd, J = 15.0 Hz, J = 7.5 Hz, J = 6.2 Hz, 1H, 10-H), 3.46 (sextet, J = 7.5 Hz, 1H, 13-H), 3.53 (dd, J = 10.8 Hz, J = 6.0 Hz, 1H, −CH$_2$-O−), 3.67 (dd, J = 10.8 Hz, J = 3.6 Hz, 1H, −CH$_2$-O−), 3.68 (br s, 1H, −OH), 4.08 (m, 1H, >N-CH(CH$_3$)−), 5.20–5.30 (m, 4H, 11-H, 12-H, 14-H, 15-H), 5.32–5.44 (m, 4H, 5-H, 6-H, 8-H, 9-H), 5.60 (br s, 1H, > NH). ^{13}C NMR (75 MHz, CDCl$_3$) δ 173.7 (>C=O), 135.1 (C-12), 134.1 (C-14), 129.0 (C-8), 128.8 (C-5), 128.4 (C-6), 128.2 (C-15), 128.1 (C-9), 125.6 (C-11), 67.4 (−CH$_2$-OH), 47.8 (−NH-CH<), 36.1 (C-2), 31.6 (C-18), 30.5 (C-13), 29.5 (C-17), 27.5 (C-16), 26.6 (C-4), 25.8 (C-10), 25.6 (C-7), 25.5 (C-3), 22.6 (C-19), 22.0 (C-13-CH_3), 17.1 (−NH-CH(CH_3)−), 14.1 (C-20). Mass spectrum (EI) m/z (relative intensity) 376 (M + H$^+$, 1), 375 (M$^+$, 2), 357 (5), 342 (7), 232 (8), 192 (12), 152 (15), 139 (22), 112 (39), 99 (100). Exact mass (EI) calculated for C$_{24}$H$_{42}$NO$_2$ (M + H$^+$) 376.3216, found 376.3213. Mass spectrum (ESI) m/z (relative intensity) 376 (M + H$^+$, 100), 339 (15), 301 (11), 269 (13). Exact mass (ESI) calculated for C$_{24}$H$_{42}$NO$_2$ (M + H$^+$) 376.3216, found 376.3210. LC/MS analysis (Waters MicroMass ZQ system) showed purity 98% and retention time 5.5 min for the title compound.

(13S,5Z,8Z,11Z,14Z)-N-((R)-1-Hydroxypropan-2-yl)-13-methyl-18-phenoxyoctadeca-5,8,11,14-tetraenamide (3b). The synthesis was carried out as described for **3a**, using **37b** (22 mg, 0.036 mmol) and TBAF (0.045 mL, 1 M solution in THF) in dry THF (0.7 mL). The reaction was completed in 1.5 h, and the crude oil obtained after work up was purified by flash column chromatography on silica gel (57:40:3 ethyl acetate:hexane:MeOH) to give **3b** (12 mg, 85% yield) as a colorless oil. ^{1}H NMR (600 MHz, CDCl$_3$) δ 0.99 (d, J = 7.2 Hz, 3H, = CH-CH(CH_3)−), 1.15 (d, J = 6.6 Hz, 3H, >N-CH(CH_3)−), 1.71 (quintet, J = 7.2 Hz, 2H, 3-H), 1.85 (m, 2H, 17-H), 2.10 (dt, J = 6.6 Hz, J = 6.6 Hz, 2H, 4-H), 2.17 (t, J = 7.2 Hz, 2H, 2-H), 2.20–2.26 (m, 1H, 16-H), 2.26–2.34 (m, 1H, 16-H), 2.75–2.85 (ddd and t, overlapping, 3H, 10-H and 7-H, especially 2.80, t, J = 6.0 Hz, 2H, 7-H), 2.87 (ddd, J = 15.6 Hz, J = 7.5 Hz, J = 6.5 Hz, 1H, 10-H), 3.49 (ddq as sextet, J = 7.2 Hz, 1H, 13-H), 3.51 (dd, J = 10.8 Hz, J = 6.3 Hz, 1H, −CH$_2$-OH), 3.65 (dd, J = 10.8 Hz, J = 3.3 Hz, 1H, −CH$_2$-OH), 3.96 (t, J = 6.6 Hz, 2H, 18-H), 4.06 (m, 1H, >N-CH(CH$_3$)−), 5.20–5.42 (m, 8H, 5-H, 6-H, 8-H, 9-H, 11-H, 12-H, 14-H, 15-H), 5.57 (br s, 1H, >NH), 6.89 (d, J = 7.4 Hz, 2H, 2-H, 6-H, −OPh), 6.93 (t, J = 7.4 Hz, 1H, 4-H, −OPh), 7.27 (t, J = 7.4 Hz, 2H, 3-H, 5-H, −OPh). ^{13}C NMR (75 MHz, CDCl$_3$) δ 173.7 (>C=O), 159.0 (C-1′,

Ar), 135.3, 134.8, 129.4 (C-3′, C-5′, Ar), 129.1, 128.8, 128.3, 128.1, 126.8, 125.8, 120.5 (C-4′, Ar), 114.5 (C-2′, C-6′, Ar), 67.5 ($-CH_2O-$), 67.0 ($-CH_2O-$), 47.8 ($-NH-CH<$), 36.0 (C-2), 30.5, 29.2, 26.6, 25.8, 25.6, 25.4, 24.0, 21.9, 17.0 ($-NH-CH(CH_3)-$). Mass spectrum (EI) *m/z* (relative intensity) 439 (M^+, 4), 421 (15), 406 (8), 328 (9), 300 (8), 232 (13), 192 (14), 152 (19), 139 (35), 112 (37), 99 (100). Exact mass (EI) calculated for $C_{28}H_{41}NO_3$ 439.3086, found 439.3083. LC/MS analysis (Waters MicroMass ZQ system) showed purity 97% and retention time 5.2 min for the title compound.

(13R,5Z,8Z,11Z,14Z)-N-((R)-1-Hydroxypropan-2-yl)-13-methyleicosa-5,8,11,14-tetraenamide (3c). The synthesis was carried out as described for **3a**, using **37c** (14 mg, 0.023 mmol) and TBAF (0.03 mL, 0.03 mmol, 1 M solution in THF) in dry THF (0.5 mL). The reaction was completed in 1.5 h, and the crude product obtained after work up was purified by flash column chromatography on silica gel (57:40:3 ethyl acetate:hexane:MeOH) to give **3c** (7 mg, 80% yield) as a colorless oil. IR (neat): 3304, 3013, 2927, 2857, 1653 (C=O), 1543, 1275, 1261, 1066 cm^{-1}. ^{1}H NMR (600 MHz, CDCl$_3$) δ 0.89 (t, *J* = 6.7 Hz, 3H, 20-H), 1.02 (d, *J* = 6.6 Hz, 3H, =CH-CH(C*H*$_3$)−), 1.17 (d, *J* = 6.6 Hz, 3H, >N-CH(C*H*$_3$)−), 1.24–1.32 (m, 4H, 18-H, 19-H), 1.35 (sextet, *J* = 7.2 Hz, 2H, 17-H), 1.72 (quintet, *J* = 7.2 Hz, 2H, 3-H), 2.06 (nonet, *J* = 6.2 Hz, 2H, 16-H), 2.12 (dt, *J* = 7.2 Hz, *J* = 7.2 Hz, 2H, 4-H), 2.20 (t, *J* = 7.8 Hz, 2H, 2-H), 2.79–2.85 (ddd and t, overlapping, 3H, 10-H and 7-H, especially 2.81, t, *J* = 6.0 Hz, 2H, 7-H), 2.87 (ddd, *J* = 15.0 Hz, *J* = 7.5 Hz, *J* = 6.2 Hz, 1H, 10-H), 3.46 (sextet, *J* = 7.5 Hz, 1H, 13-H), 3.53 (dd, *J* = 10.8 Hz, *J* = 6.0 Hz, 1H, −CH$_2$-O−), 3.67 (dd, *J* = 10.8 Hz, *J* = 3.6 Hz, 1H, −CH$_2$-O−), 3.68 (br s, 1H, −OH), 4.08 (m, 1H, >N-C*H*(CH$_3$)−), 5.20–5.31 (m, 4H, 11-H, 12-H, 14-H, 15-H), 5.32–5.44 (m, 4H, 5-H, 6-H, 8-H, 9-H), 5.55 (br s, 1H, >NH). ^{13}C NMR (75 MHz, CDCl$_3$) δ 173.7 (>C=O), 135.1 (C-12), 134.1 (C-14), 129.0 (C-8), 128.8 (C-5), 128.4 (C-6), 128.2 (C-15), 128.1 (C-9), 125.6 (C-11), 67.4 ($-CH_2$-OH), 47.8 ($-NH-CH<$), 36.1 (C-2), 31.6 (C-18), 30.5 (C-13), 29.4 (C-17), 27.5 (C-16), 26.6 (C-4), 25.8 (C-10), 25.6 (C-7), 25.5 (C-3), 22.6 (C-19), 22.0 (C-13-*CH*$_3$), 17.1 ($-NH-CH(CH_3)-$), 14.1 (C-20). MS (EI): *m/z* (%): 375 (M^+, 1), 374 (2), 312 (11), 284 (17), 257 (23), 244 (30), 171 (41), 57 (100). Exact mass (EI) calculated for $C_{24}H_{41}NO_2$ 375.3137, found 375.3128. MS (ESI): *m/z* (%): 376 ($M + H^+$, 52), 339 (84), 269 (100). Exact mass (ESI) calculated for $C_{24}H_{42}NO_2$ ($M + H^+$) 376.3216, found 376.3203. LC/MS analysis (Waters MicroMass ZQ system) showed purity 98% and retention time 5.5 min for the title compound.

(7R,5Z,8Z,11Z,14Z)-N-((R)-1-Hydroxypropan-2-yl)-7-methyleicosa-5,8,11,14-tetraenamide (3d). The synthesis was carried out as described for **3a**, using **37d** (20 mg, 0.032 mmol) and TBAF (0.03 mL, 0.03 mmol, 1 M solution in THF) in dry THF (0.5 mL). The reaction was completed in 1.5 h, and the crude product obtained after work up was purified by flash column chromatography on silica gel (57:40:3 ethyl acetate:hexane:MeOH) to give **3d** (10 mg, 85% yield) as a colorless oil. IR (neat): 3302, 3011, 2927, 2857, 1647 (C=O), 1542, 1270, 1261, 1061 cm^{-1}. ^{1}H NMR (500 MHz, CDCl$_3$) δ 0.89 (t, *J* = 6.9 Hz, 3H, 20-H), 1.02 (d, *J* = 6.7 Hz, 3H, =CH-CH(C*H*$_3$)−), 1.17 (d, *J* = 6.7 Hz, 3H, >CH-C*H*$_3$), 1.23–1.42 (m, 6H, 17-H, 18-H, 19-H), 1.67–1.78 (quintet, *J* = 7.0 Hz, 2H, 3-H), 2.06 (dt, *J* = 7.0 Hz, *J* = 7.0 Hz, 2H, 16-H), 2.09–2.17 (m, 2H, 4-H), 2.19 (t, *J* = 7.5 Hz, 2H, 2-H), 2.75–2.91 (m, 4H, 10-H, 13-H), 3.44 (sextet, *J* = 7.0 Hz, 1H, 7-H), 3.53 (m as qtd, *J* = 10.8 Hz, *J* = 3.7 Hz, 1H, −C*H*$_2$OH), 3.66 (m as br d, *J* = 10.8 Hz, 1H, −C*H*$_2$OH), 4.07 (m, 1H, >C*H*(CH$_3$)), 5.20–5.45 (m, 8H, 5-H, 6-H, 8-H, 9-H, 11-H, 12-H, 14-H, 15-H), 5.56 (br d, *J* = 5.3 Hz, 1H, >NH). ^{13}C NMR (100 MHz, CDCl$_3$) δ 173.6 (C=O),

135.3 (C=C), 134.7 (C=C), 130.5 (C=C), 128.6 (C=C), 128.0 (C=C), 127.5 (C=C), 126.8 (C=C), 125.9 (C=C), 67.5 (CH_2OH), 47.9 (−NHCH<), 36.1, 31.5, 30.5, 29.3, 27.2, 26.9, 25.8, 25.6, 25.5, 22.5, 22.0, 17.0, 14.0. Mass spectrum (ESI) m/z (relative intensity) 377 (M^+ + 2H, 25), 376 (M^+ + H, 100), 301 (8). Exact mass (ESI) calculated for $C_{24}H_{42}NO_2$ (M^+ + H) 376.3216, found 376.3208. LC/MS analysis (Waters MicroMass ZQ system) showed purity 98% and retention time 5.5 min for the title compound.

(7S,5Z,8Z,11Z,14Z)-N-((R)-1-Hydroxypropan-2-yl)-7-methyleicosa-5,8,11,14-tetraenamide **(3e).** The synthesis was carried out as described for **3a**, using **37e** (20 mg, 0.032 mmol) and TBAF (0.03 mL, 0.03 mmol, 1 M solution in THF) in dry THF (0.5 mL). The reaction was completed in 1.5 h, and the crude product obtained after work up was purified by flash column chromatography on silica gel (57:40:3 ethyl acetate:hexane:MeOH) to give **3e** (10 mg, 81% yield) as a colorless oil. IR (neat): 3304, 3012, 2927, 2857, 1650 (C=O), 1543, 1278, 1264, 1059 cm^{-1}. ^{1}H NMR (500 MHz, $CDCl_3$) δ 0.89 (t, J = 6.9 Hz, 3H, 20-H), 1.02 (d, J = 6.7 Hz, 3H, =CH-CH(CH_3)−), 1.17 (d, J = 6.7 Hz, 3H, >CH-CH_3), 1.23–1.42 (m, 6H, 17-H, 18-H, 19-H), 1.67–1.78 (quintet, J = 7.0 Hz, 2H, 3-H), 2.06 (dt, J = 7.0 Hz, J = 7.0 Hz, 2H, 16-H), 2.09–2.17 (m, 2H, 4-H), 2.19 (t, J = 7.5 Hz, 2H, 2-H), 2.75–2.91 (m, 4H, 10-H, 13-H), 3.44 (sextet, J = 7.0 Hz, 1H, 7-H), 3.53 (m as qtd, J = 10.8 Hz, J = 3.7 Hz, 1H, −CH_2OH), 3.66 (m as br d, J = 10.8 Hz, 1H, −CH_2OH), 4.07 (m, 1H, >CH(CH_3)), 5.20–5.45 (m, 8H, 5-H, 6-H, 8-H, 9-H, 11-H, 12-H, 14-H, 15-H), 5.56 (br d, J = 5.3 Hz, 1H, >NH). ^{13}C NMR (100 MHz, $CDCl_3$) δ 173.7 (C=O), 135.4 (C=C), 134.7 (C=C), 130.6 (C=C), 128.6 (C=C), 128.0 (C=C), 127.5 (C=C), 126.8 (C=C), 125.9 (C=C), 67.5 (CH_2OH), 47.9 (NHCH), 36.2, 31.5, 30.5, 29.3, 27.2, 26.9, 25.8, 25.6, 25.6, 22.5, 22.0, 17.0, 14.0. Mass spectrum (ESI) m/z (relative intensity) 398 (M^+ + Na, 8), 376 (M^+ + H, 100), 301 (8). Exact mass (ESI) calculated for $C_{24}H_{42}NO_2$ (M^+ + H) 376.3216, found 376.3206. LC/MS analysis (Waters MicroMass ZQ system) showed purity 98% and retention time 5.5 min for the title compound.

(13S,5Z,8Z,11Z,14Z)-N-Cyclopropyl-13-methyleicosa-5,8,11,14-tetraenamide **(4a).** A solution of (13*S*,5*Z*,8*Z*,11*Z*,14*Z*)-13-methyleicosa-5,8,11,14-tetraenoic acid (**34a**, 12 mg, 0.04 mmol) and dried carbonyldiimidazole (18 mg, 0.113 mmol) in dry THF (0.63 mL) at room temperature under an argon atmosphere was stirred for 2 h, and then a solution of cyclopropyl amine (9 mg, 0.151 mmol) in THF (0.2 mL) was added. The reaction mixture was stirred for 1 h and then diluted with water and ethyl acetate. The organic phase was separated, and the aqueous phase extracted with AcOEt. The combined organic layer was washed with brine, dried over $MgSO_4$, and concentrated under reduced pressure. Purification by flash column chromatography on silica gel (25% acetone in hexane) gave 12 mg (91% yield) of **4a** as a colorless oil. ^{1}H NMR (500 MHz, $CDCl_3$) δ 0.47 (m, 2H of the cyclopropyl ring), 0.76 (m, 2H of the cyclopropyl ring), 0.89 (t, J = 6.9 Hz, 3H, 20-H), 1.02 (d, J = 6.6 Hz, 3H, >CH-CH_3), 1.24–1.33 (m, 4H, 18-H, 19-H), 1.35 (sextet, J = 7.2 Hz, 2H, 17-H), 1.71 (quintet, J = 7.2 Hz, 2H, 3-H), 2.02–2.09 (m, 2H, 16-H), 2.10 (dt, J = 7.2 Hz, J = 7.2 Hz, 2H, 4-H), 2.12 (t, J = 7.8 Hz, 2H, 2-H), 2.70 (octet, J = 3.6 Hz, 1H, >N-CH<), 2.75–2.85 (ddd and t overlapping, 3H, 10-H and 7-H, especially 2.80, t, J = 6.6 Hz, 2H, 7-H), 2.87 (ddd, J = 15.0 Hz, J = 7.3 Hz, J = 6.6 Hz, 1H, 10-H), 3.46 (sextet, J = 7.5 Hz, 1H, 13-H), 5.20–5.30 (m, 4H, 11-H, 12-H, 14-H, 15-H), 5.31–5.43 (m, 4H, 5-H, 6-H, 8-H, 9-H), 5.51 (br s, 1H, >NH). ^{13}C NMR (100 MHz, $CDCl_3$) δ 174.1 (C=O), 135.1 (C=C), 134.1 (C=C), 129.1 (C=C), 128.7 (C=C), 128.4 (C=C), 128.2 (C=C), 128.1 (C=C), 125.6 (C=C), 35.9 (−NH-CH<), 31.5, 30.5, 29.4, 27.5, 26.6, 25.8, 25.6, 25.4, 22.5, 22.0, 14.0, 6.6. Mass

spectrum (EI) *m/z* (relative intensity) 357 (M$^+$, 5), 300 (4), 286 (5), 232 (10), 117 (7), 175 (11), 147 (10), 133 (17), 119 (17), 107 (22), 99 (39), 93 (54), 57 (100). Exact mass (EI) calculated for C$_{24}$H$_{39}$NO 357.3032, found 357.3025. LC/MS analysis (Waters MicroMass ZQ system) showed purity 97% and retention time 6.1 min for the title compound.

(13S,5Z,8Z,11Z,14Z)-N-Cyclobutyl-13-methyleicosa-5,8,11,14-tetraenamide **(4b).** The synthesis was carried out as described for **4a**, using **34a** (24 mg, 0.08 mmol), fresh carbonyldiimidazole (37 mg, 0.226 mmol), and cyclobutyl amine (22 mg, 0.302 mmol) in dry THF (0.4 mL). The crude oil obtained after work up was purified by flash column chromatography on silica gel (16% acetone in hexane) and gave **4b** (26 mg, 92% yield) as a colorless oil. ^{1}H NMR (600 MHz, CDCl$_3$) δ 0.89 (t, *J* = 6.9 Hz, 3H, 20-H), 1.02 (d, *J* = 6.6 Hz, 3H, >CH-C*H*$_3$), 1.25–1.33 (m, 4H, 18-H, 19-H), 1.36 (sextet, *J* = 7.2 Hz, 2H, 17-H), 1.65–1.74 (m and quintet overlapping, 4H, cyclobutane ring and 3-H, especially 1.71, quintet, *J* = 7.2 Hz, 2H, 3-H), 1.78–1.86 (m, 2H, cyclobutane ring), 2.03–2.09 (m, 2H, 16-H), 2.10 (dt, *J* = 7.2 Hz, *J* = 7.2 Hz, 2H, 4-H), 2.13 (t, *J* = 7.2 Hz, 2H, 2-H), 2.30–2.38 (m, 2H, cyclobutane ring), 2.75–2.85 (ddd and t overlapping, 3H, 10-H and 7-H, especially 2.80, t, *J* = 6.2 Hz, 2H, 7-H), 2.87 (ddd, *J* = 15.0 Hz, *J* = 7.4 Hz, *J* = 6.7 Hz, 1H, 10-H), 3.46 (sextet, *J* = 7.7 Hz, 1H, 13-H), 4.10 (sextet, *J* = 8.4 Hz, 1H, >N-CH<), 5.20–5.30 (m, 4H, 11-H, 12-H, 14-H, 15-H), 5.31–5.43 (m, 4H, 5-H, 6-H, 8-H, 9-H), 5.52 (br s, 1H, >NH). ^{13}C NMR (75 MHz, CDCl$_3$) δ 171.8 (>C=O), 135.1 (C-12), 134.1 (C-14), 129.1 (C-8), 128.7 (C-5), 128.4 (C-6), 128.2 (C-15), 128.1 (C-9), 125.6 (C-11), 44.6 (−NH-CH<), 36.0 (C-2), 31.6 (C-18), 31.4 (cyclobutane ring), 30.5 (C-13), 29.4 (C-17), 27.5 (C-16), 26.6 (C-4), 25.8 (C-10), 25.6 (C-7), 25.4 (C-3), 22.6 (C-19), 22.0 (C-13-C*H*$_3$), 15.0 (cyclobutane ring), 14.1 (C-20). Mass spectrum (ESI) *m/z* (relative intensity) 372 (M + H$^+$, 100), 301 (5). Exact mass (ESI) calculated for C$_{25}$H$_{42}$NO (M + H$^+$) 372.3266, found 372.3264. LC/MS analysis (Waters MicroMass ZQ system) showed purity 98% and retention time 6.1 min for the title compound.

(13S,5Z,8Z,11Z,14Z)-N-Cyclopentyl-13-methyleicosa-5,8,11,14-tetraenamide **(4c).** The synthesis was carried out as described for **4a**, using **34a** (24 mg, 0.08 mmol), fresh carbonyldiimidazole (37 mg, 0.226 mmol), and cyclopentyl amine (26 mg, 0.302 mmol) in dry THF (0.4 mL). The crude oil obtained after work up was purified by flash column chromatography on silica gel (20% acetone in hexane) and gave **4c** (25 mg, 85% yield) as a colorless oil. ^{1}H NMR (600 MHz, CDCl$_3$) δ 0.88 (t, *J* = 7.2 Hz, 3H, 20-H), 1.02 (d, *J* = 6.6 Hz, 3H, >CH-C*H*$_3$), 1.24–1.39 (m, 8H, cyclopentane ring, 17-H, 18-H, 19-H), 1.56–1.62 (m, 2H, cyclopentane ring), 1.62–1.69 (m, 2H, cyclopentane ring), 1.70 (quintet, *J* = 7.5 Hz, 2H, 3-H), 1.99 (sextet, *J* = 6.3 Hz, 2H, cyclopentane ring), 2.03–2.09 (m, 2H, 16-H), 2.11 (dt, *J* = 7.3 Hz, *J* = 7.3 Hz, 2H, 4-H), 2.14 (t, *J* = 7.8 Hz, 2H, 2-H), 2.75–2.85 (ddd and t overlapping, 3H, 10-H and 7-H, especially 2.80, t, *J* = 6.0 Hz, 2H, 7-H), 2.87 (ddd, *J* = 15.0 Hz, *J* = 7.4 Hz, *J* = 6.7 Hz, 1H, 10-H), 3.46 (sextet, *J* = 7.8 Hz, 1H, 13-H), 4.21 (sextet, *J* = 7.2 Hz, 1H, >N-CH<), 5.20–5.30 (m, 4H, 11-H, 12-H, 14-H, 15-H), 5.31–5.43 (m, 5H, >NH, 5-H, 6-H, 8-H, 9-H). ^{13}C NMR (75 MHz, CDCl$_3$) δ 172.32 (>C=O), 135.1 (C-12), 134.1 (C-14), 129.2 (C-8), 128.7 (C-5), 128.4 (C-6), 128.2 (C-15), 128.1 (C-9), 125.6 (C-11), 51.1 (−NH-CH<), 36.2 (C-2), 33.2 (cyclopentane ring), 31.6 (C-18), 30.5 (C-13), 29.4 (C-17), 27.5 (C-16), 26.6 (C-4), 25.8 (C-10), 25.6 (C-7 or C-3), 25.6 (C-3 or C-7), 23.7 (cyclopentane ring), 22.6 (C-19), 22.0 (C-13-C*H*$_3$), 14.1 (C-20). Mass spectrum (ESI) *m/z* (relative intensity) 386 (M + H$^+$, 100), 184 (9). Exact mass (ESI) calculated for C$_{26}$H$_{44}$NO (M + H$^+$) 386.3423, found 386.3414. LC/MS analysis (Waters MicroMass ZQ system) showed purity 98% and retention time 6.1 min for the title compound.

(13S,5Z,8Z,11Z,14Z)-13-Methyl-N-(prop-2-yn-1-yl)eicosa-5,8,11,14-tetraenamide **(4d).** The synthesis was carried out as described for **4a**, using **34a** (12 mg, 0.04 mmol), fresh carbonyldiimidazole (18 mg, 0.113 mmol), and propargyl amine (8.3 mg, 0.151 mmol) in dry THF (0.2 mL). The crude oil obtained after work up was purified by flash column chromatography on silica gel (25% acetone in hexane) and gave **4d** (12 mg, 88% yield) as a colorless oil. ^{1}H NMR (600 MHz, CDCl$_3$) δ 0.89 (t, J = 6.6 Hz, 3H, 20-H), 1.02 (d, J = 6.6 Hz, 3H, >CH-CH_3), 1.24–1.33 (m, 4H, 18-H, 19-H), 1.37 (sextet, J = 7.2 Hz, 2H, 17-H), 1.73 (quintet, J = 7.8 Hz, 2H, 3-H), 2.06 (nonet, J = 7.2 Hz, 2H, 16-H), 2.12 (dt, J = 7.2 Hz, J = 7.2 Hz, 2H, 4-H), 2.20 (t, J = 7.8 Hz, 2H, 2-H), 2.23 (t, J = 2.4 Hz, 1H, −C≡CH), 2.75–2.84 (ddd and t overlapping, 3H, 10-H and 7-H, especially 2.81, t, J = 6.0 Hz, 2H, 7-H), 2.87 (ddd, J = 15.0 Hz, J = 7.5 Hz, J = 6.2 Hz, 1H, 10-H), 3.46 (sextet, J = 7.8 Hz, 1H, 13-H), 4.05 (dd, J = 4.8 Hz, J = 2.4 Hz, 2H, −CH$_2$-C≡C−), 5.20–5.30 (m, 4H, 11-H, 12-H, 14-H, 15-H), 5.32–5.44 (m, 4H, 5-H, 6-H, 8-H, 9-H), 5.55 (br s, 1H, >NH). ^{13}C NMR (75 MHz, CDCl$_3$) δ 172.3 (>C=O), 135.1 (C-12), 134.1 (C-14), 128.9 (C-8), 128.9 (C-5), 128.4 (C-6), 128.2 (C-15), 128.1 (C-9), 125.6 (C-11), 79.5 (−C≡CH), 71.6 (−C≡CH), 35.7 (C-2), 31.5 (C-18), 30.5 (C-13), 29.4 (C-17), 29.1 (−NH-CH$_2$−), 27.5 (C-16), 26.5 (C-4), 25.8 (C-10), 25.6 (C-7), 25.2 (C-3), 22.6 (C-19), 22.0 (C-13-CH$_3$), 14.0 (C-20). Mass spectrum (ESI) *m/z* (relative intensity) 356 (M + H$^+$, 100), 301 (10). Exact mass (ESI) calculated for C$_{24}$H$_{38}$NO (M + H$^+$) 356.2953, found 356.2953. LC/MS analysis (Waters MicroMass ZQ system) showed purity 98% and retention time 6.0 min for the title compound.

(13S,5Z,8Z,11Z,14Z)-N-(2-Chloroethyl)-13-methyleicosa-5,8,11,14-tetraenamide **(4e).** The synthesis was carried out as described for **4a**, using **34a** (25 mg, 0.08 mmol), fresh carbonyldiimidazole (38 mg, 0.236 mmol), and a mixture of chloroethyl amine hydrochloride 37 mg, 0.314 mmol) and dry pyridine (0.3 mL) in THF (0.4 mL). The crude oil obtained after work up was purified by flash column chromatography on silica gel (20% acetone in hexane) and gave **4e** (27 mg, 89% yield) as a colorless oil. ^{1}H NMR (600 MHz, CDCl$_3$) δ 0.89 (t, J = 6.7 Hz, 3H, 20-H), 1.02 (d, J = 6.6 Hz, 3H, >CH-CH_3), 1.24–1.33 (m, 4H, 18-H, 19-H), 1.36 (sextet, J = 7.2 Hz, 2H, 17-H), 1.73 (quintet, J = 7.8 Hz, 2H, 3-H), 2.06 (nonet, J = 6.6 Hz, 2H, 16-H), 2.12 (dt, J = 7.2 Hz, J = 7.2 Hz, 2H, 4-H), 2.22 (t, J = 7.8 Hz, 2H, 2-H), 2.76–2.84 (ddd and t overlapping, 3H, 10-H and 7-H, especially 2.81, t, J = 6.0 Hz, 2H, 7-H), 2.87 (ddd, J = 15.0 Hz, J = 7.5 Hz, J = 6.2 Hz, 1H, 10-H), 3.46 (sextet, J = 7.4 Hz, 1H, 13-H), 3.58–3.65 (m and t overlapping, 4H, >N-CH_2−, −CH_2-Cl, especially 3.62, t, J = 4.8 Hz, 2H, −CH_2-Cl), 5.20–5.31 (m, 4H, 11-H, 12-H, 14-H, 15-H), 5.33–5.44 (m, 4H, 5-H, 6-H, 8-H, 9-H), 5.84 (br s, 1H, >NH). ^{13}C NMR (75 MHz, CDCl$_3$) δ 173.0 (>C=O), 135.1 (C-12), 134.1 (C-14), 129.0 (C-8), 128.9 (C-5), 128.4 (C-6), 128.2 (C-15), 128.1 (C-9), 125.6 (C-11), 44.2 (−CH$_2$Cl), 41.1 (−NH-CH$_2$−), 35.9 (C-2), 31.6 (C-18), 30.5 (C-13), 29.5 (C-17), 27.5 (C-16), 26.6 (C-4), 25.8 (C-10), 25.6 (C-7), 25.4 (C-3), 22.6 (C-19), 22.0 (C-13-CH$_3$), 14.0 (C-20). Mass spectrum (ESI) *m/z* (relative intensity) 380 (M + H$^+$, 100), 338 (15), 216 (12), 178 (15). Exact mass (ESI) calculated for C$_{23}$H$_{39}$ClNO (M + H$^+$) 380.2720, found 380.2703. LC/MS analysis (Waters MicroMass ZQ system) showed purity 98% and retention time 5.8 min for the title compound.

(13S,5Z,8Z,11Z,14Z)-20-Azido-N-cyclopropyl-13-methyleicosa-5,8,11,14-tetraenamide **(4f).** A solution of acid **44** (75 mg, 0.209 mmol) and dried carbonyldiimidazole (96 mg, 0.593 mmol) in dry THF (6.7 mL) at room temperature under an argon atmosphere was stirred for 2 h, and then

cyclopropylamine (0.089 mL, 2.965 mmol) was added. The reaction mixture was stirred for 2 h and then diluted with water and ethyl acetate. The organic phase was separated, and the aqueous phase extracted with EtOAc. The combined organic layer was washed with brine, dried over $MgSO_4$, and concentrated under reduced pressure. The crude product obtained after work up was purified by flash column chromatography on silica gel (59:40:1 EtOAc:hexane:MeOH) and gave 62 mg (74% yield) of **4f** as a colorless oil. IR (neat) 3276 (br, OH), 2927, 2093 (s, N_3), 1645, 1541, 1454, 1261, 720 cm^{-1}. ^{1}H NMR (500 MHz, CDCl$_3$) δ 0.45–0.50 (m, 2H, cyclopropyl ring), 0.73–0.79 (m, 2H, cyclopropyl ring), 1.01 (d, J = 6.5 Hz, 3H, >CH-CH_3), 1.34–1.42 (m, 4H, 18-H, 19-H), 1.60 (br quintet, J = 7.0 Hz, 2H, 17-H), 1.71 (quintet, J = 7.5 Hz, 2H, 3-H), 2.07–2.14 (m, 6H, 2-H, 4-H and 16-H), 2.66–2.72 (m, 1H, −NH-CH<), 2.78–2.88 (m, 4H, 7-H, 10-H), 3.26 (t, J = 6.5 Hz, 2H, 20-H), 3.46 (ddq as sextet, J = 7.5 Hz, 1H, 13-H), 5.20–5.30 (m, 4H, 11-H, 12-H, 14-H, 15-H), 5.32–5.43 (m, 4H, 5-H, 6-H, 8-H, 9-H), 5.55 (br s, 1H, >NH). ^{13}C NMR (100 MHz, CDCl$_3$) δ 174.1 (>C=O), 134.9 (−CH=), 134.6 (−CH=), 129.1 (−CH=), 128.7 (−CH=), 128.3 (−CH=), 128.2 (−CH=), 127.6 (−CH=), 125.7 (−CH=), 51.4, 35.8, 30.5, 29.7, 29.2, 28.8, 27.3, 26.6, 26.4, 25.8, 25.6, 25.4, 22.5, 22.0 (C_{13}-Me), 6.61. Mass spectrum (ESI) m/z (relative intensity) 400 (M$^+$ + H + 1, 27), 399 (M$^+$ + H, 100), 372 (M$^+$ + H + 1-N$_2$, 20), 371 (M$^+$ + H − N$_2$, 71). Exact mass (ESI) calculated for $C_{24}H_{39}N_4O$ (M$^+$ + H) 399.3124, found 399.3122. LC/MS analysis (Waters MicroMass ZQ system) showed purity 98% and retention time 5.9 min for the title compound.

(13S,5Z,8Z,11Z,14Z)-N-Cyclopropyl-20-isothiocyanato-13-methyleicosa-5,8,11,14-tetraenamide (4g). To a solution of **4f** (30 mg, 0.074 mmol) in anhydrous THF (2 mL) was added triphenyl phosphine (58 mg, 0.222 mmol) and carbon disulfide (53 mg, 0.74 mmol), and the reaction mixture was stirred at room temperature for 48 h. After completion, the reaction mixture was concentrated under vacuum and purified by flash column chromatography on silica gel (59:40:1 EtOAc:hexane:MeOH) and gave 30 mg of **4g** as a viscous oil in 96% yield. IR (neat) 3273, 2926, 2091 (s, NCS), 1643, 1536, 1453, 1347, 1021 cm^{-1}. ^{1}H NMR (500 MHz, CDCl$_3$) δ 0.45–0.50 (m, 2H, cyclopropyl ring), 0.73–0.79 (m, 2H, cyclopropyl ring), 1.01 (d, J = 6.5 Hz, 3H, >CH-CH_3), 1.34–1.42 (m, 4H, 18-H, 19-H), 1.60 (br quintet, J = 7.0 Hz, 2H, 17-H), 1.71 (quintet, J = 7.5 Hz, 2H, 3-H), 2.07–2.14 (m, 6H, 2-H, 4-H and 16-H), 2.66–2.72 (m, 1H, −NH-CH<), 2.78–2.88 (m, 4H, 7-H, 10-H), 3.46 (ddq as sextet, J = 7.5 Hz, 1H, 13-H), 3.51 (t, J = 6.5 Hz, 2H, 20-H), 5.20–5.30 (m, 4H, 11-H, 12-H, 14-H, 15-H), 5.32–5.43 (m, 4H, 5-H, 6-H, 8-H, 9-H), 5.55 (br s, 1H, >NH). ^{13}C NMR (100 MHz, CDCl$_3$) δ 174.1 (>C=O), 134.9 (C=C), 134.8 (C=C), 129.1 (C=C), 128.7 (C=C), 128.3 (C=C), 128.2 (C=C), 127.4 (C=C), 125.7 (C=C), 45.0, 35.9, 30.5, 30.3, 29.9, 29.7, 28.9, 27.2, 26.6, 26.2, 25.8, 25.6, 25.4, 22.6, 22.0, 6.6. Mass spectrum (ESI) m/z (relative intensity) 416 (M$^+$ + H + 1, 28), 415 (M$^+$ + H, 100), 358 (8). Exact mass (ESI) calculated for $C_{25}H_{39}N_2OS$ (M$^+$ + H), 413.3056, found 413.3043. LC/MS analysis (Waters MicroMass ZQ system) showed purity 97% and retention time 5.8 min for the title compound.

Radioligand Binding Assays. The affinities (K_i) of the new compounds for rat CB1 receptor as well as for mouse and human CB2 receptors were obtained by using membrane preparations from rat brain or HEK293 cells expressing either mCB2 or hCB2 receptors, and [^{3}H]CP-55,940 as the radioligand, as previously described.[6,26] Membrane pretreatment with PMSF was carried out as in our earlier work.[6] Results from the competition assays were analyzed using nonlinear regression to determine the IC$_{50}$ values for the ligand.[33] K_i values were calculated from the IC$_{50}$ (Prism by GraphPad Software, Inc.). Each experiment was performed in triplicate

and K_i values determined from three independent experiments and are expressed as the mean of the three values.

cAMP Assay. HEK293 cells stably expressing rCB1 receptors were used for the studies.[27,34] The cAMP assay was carried out using PerkinElmer's Lance Ultra cAMP kit following the protocol of the manufacturer. Briefly, the assays were carried out in 384-well plates using 1000–1500 cells/well. The cells were harvested with nonenzymatic cell dissociation reagent Versene, washed once with HBSS, and resuspended in the stimulation buffer. The various concentrations of the test compound (5 µL) in forskolin (2 µM final concentration) containing stimulation buffer were added to the plate followed by the cell suspension (5 µL). Cells were stimulated for 30 min at room temperature. Eu-cAMP tracer working solution (5 µL) and Ulight-anti-cAMP working solution (5 µL) were then added to the plate and incubated at room temperature for 60 min. The data were collected on a PerkinElmer Envision instrument. The EC_{50} values were determined by nonlinear regression analysis using GraphPad Prism software (GraphPad Software, Inc., San Diego, CA).

Stability in Human (h) and Rat (r) FAAH. We have preparations of expressed, purified rat (r), and human (h) FAAH for enzyme assays currently performed in our lab.[35,36] FAAH is incubated with individual compounds or native substrate (AEA) for comparison for 30 min. Samples taken at various time points are diluted with acetonitrile to precipitate the proteins for LC-MS/MS analysis.[37,38] For samples analyzed by LC-MS/MS, chromatographic separation was achieved using an Agilent Zorbax SB-CN column (2.1 mm × 50 mm, 5 mm) on a Finnigan TSQ Quantum Ultra triple quad mass spectrometer (Thermo Electron, San Jose CA) with an Agilent 1100 HPLC on the front end (Agilent Technologies, Wilmington DE) as previously described.[39] The mobile phase consisted of 10 mM ammonium acetate, pH 7.3 (A) and methanol (B) in a flow rate of 0.5 mL/min; the autosampler was kept at 4 °C to prevent analyte degradation. Eluted peaks were ionized via atmospheric pressure chemical ionization (APCI) in MRM mode. Internal standards were used to quantify the analyte concentrations.

Stability in hMGL and hABHD6. *Cloning and Expression of hMGL and hABHD6 Proteins in E. coli Cells.* hMGL and hABHD6 were expressed in BL21 (DE3) *Escherichia coli* cells following genes cloning into pET45 vector as we described earlier.[40] Briefly, a single *E. coli* BL21 (DE3) colony containing the plasmids with hMGL or hABHD6 gene was inoculated into 10 mL of Luria broth supplemented with ampicillin (100 µg mL^{-1}) and grown overnight at 30 °C for hMGL and 37 °C for hABHD6 with shaking (250 rpm). The next morning, these 10 mL mixtures were used to inoculate 500 mL of fresh Luria broth–ampicillin medium and allowed to grow under the specified conditions (30 °C for hMGL and 20 °C for hABHD6) until the culture reached an OD_{600} of 0.7–1.2, at which time expression was induced by adding 0.3 mM (final concentration) of isopropyl-β-d-thiogalactopyranoside. After 5–7 h induction, the cells were harvested by centrifugation, washed with PBS (phosphate-buffered saline), and either used immediately or stored at −80 °C.

Preparation of E. coli Cells Lysate Containing hMGL or hABHD6 Protein. An *E. coli* cell pellet (100 mg) containing the hMGL or hABHD6 protein was resuspended in 1 mL of lysis buffer (150 mM NaCl, 50 mM Tris, 1% Triton X-100, pH 8.0) and disrupted on ice using five, 50 s sonication cycles (1 s sonication bursts at 23 W power separated by 5 s intervals, Vibra-Cell

500W, Sonics, Newtown, CT). The lysate was rotated at 4 °C for 1 h to complete extraction and solubilization of proteins from cells debris and then centrifuged at 20000g for 10 min at 4 °C.

Stability Assay. hMGL or hABHD6 (0.5 μg of total protein) are incubated at 37 °C with AMG315 or native substrate (2-AG) for comparison for 30 min. Samples taken at various time points (0, 2, 5, 10, 15, 20, 25, and 30 min) are diluted with acetonitrile to precipitate the proteins, vortexed, and certifuged for HPLC analysis. For samples analyzed by HPLC, chromatographic separation was achieved using a Supelco Discovery C18 (4.6 mm × 250 mm) column on a Waters Alliance 2695 HPLC system. Mobile phase consisted of acetonitrile (A) and water with 5% acetonitrile (B). Gradient elution started with 5% A, transitioning to 95% A over 10 min and held for 10 min at 95% A before returning to starting conditions; run time was 23 min, the flow rate was 1 mL/min, and UV detection was at 204 nm. External standards in acetonitrile were used to quantify the analyte concentrations.

Stability in mCOX-2. We have used a polarographic assay that measures oxygen consumption to investigate the endogenous AEA and AA as well as key analogues as substrates of mCOX-2 activity.[31,41]

Enzyme Preparation. Murine cyclooxygenase-2 was expressed in baculovirus-insect cell expression system. A pvL-1393 plasmid bearing the cDNA of murine COX-2 were cotransferred with linearized BaculoGold DNA to generate the recombinant baculovirus. Protein expression was performed in Sf-9 insect cells by infection for 48 h. The cell pellets were harvested, lysed, and purified by sequential ion-exchange and size exclusion chromatography to greater than 95% purity.[41]

Oxygen Consumption Assays. Cyclooxygenase inhibition was monitored by O_2 consumption using a Clark-type O2 sensitive electrode (Hansatech Pentney, Norfolk, England). Calibration was achieved using a N_2 saturated solution to establish a zero O_2 level within the reaction chamber prior to experimental measurements. All final 1 mL assay solutions contained 50 nM purified protein, 2 equiv of hematin, 100 mM Tris-Cl pH 8.0, 5 mM phenol, and 1% DMSO. The reaction was initiated by addition of substrates or test compounds in DMSO by airtight syringes. Final concentration of substrates and test compounds were 50 μM. Oxygen consumption was monitored using a Hansatech OXYG1 plus, connected to a DW1 oxygen electrode chamber controlled with Oxyview software (PP Systems Inc., MA). The rates were calculated based on the maximal first derivate of the oxygen concentration curve and normalized to the rates of arachidonic acid.

Molecular Modeling. *Conformational Analysis.* A conformational analysis of the large number of conformations that can be adopted by the flexible molecules **3a** and **3c** was accomplished using the Conformational Memories (CM) technique.[42−44] This method is based on the exploration of the possible low-free energy conformations of a flexible ligand via Monte Carlo/simulated annealing random walks employing the CHARMM (Chemistry at Harvard Molecular Mechanics) force field. This technique overcomes energy barriers efficiently and converges in a reasonable number of steps. Through CM, a complete sampling of the conformational space of **3a** and **3c** was accomplished.

Numbering System. The Ballesteros–Weinstein numbering system has been used for numbering the corresponding GPCR amino acid residues. This numbering system is based on assignment of 0.50 to the most highly conserved residue in each transmembrane helix (TMH).[45] This number is preceded by the TMH number. According to this system, for instance, the most highly conserved residue in TMH6 is P6.50. The previous amino acid would be labeled 6.49, and the residue immediately after this would be labeled 6.51. When referring to a loop residue the absolute sequence number is given in parentheses.

Materials and Methods for Characterization of in Vivo Effects. *Subjects.* Adult male mice (39 ± 10 g) were used in this study. Wild-type CD1 mice or CB1 knockout (KO) mice on a CD1 background strain were used. Animals were single housed in a temperature-controlled facility with food and water ad libitum and maintained on a 12 h light/dark cycle. Mice were bred and genotyped in the Mackie lab. Behavioral testing was performed in the Hohmann lab. All the experimental procedures were approved by Bloomington Institutional Animal Care and Use Committee of Indiana University and followed the guidelines for the treatment of animals of the International Association for the Study of Pain (Zimmermann, 1983).

Chemicals. AMG315, AM356, and anandamide (AEA) were dissolved in a vehicle of dimethysulfoxide (Sigma-Aldrich, St. Louis, MO), emulphor (Alkamuls EL 620L, Solvay, Princeton, NJ), ethanol (Sigma-Aldrich), and sterile saline (Aquilite System, Hospira Inc., Lake Forest, IL) at a ratio of 5:2:2:16, respectively. Drugs were delivered via ip injection in a volume of 5 mL/kg.

CFA-Induced Inflammatory Nociception. A single intraplantar injection of mixed solution of complete Freund's adjuvant (CFA) and saline (at ratio of 1:1; 20 μL total volume) was delivered unilaterally into the plantar surface of the right hind paw. Animals were given 48 h to fully develop inflammatory pain before pharmacologic manipulations.

Assessment of Mechanical Allodynia. Mechanical paw withdrawal thresholds were determined as described previously.[32] Animals were habituated in Plexiglas test chambers for at least 30 min prior to the testing. An electronic von Frey anesthesiometer with 90 g probe (IITC Life Science, Woodland Hills, CA) was used to determine the paw withdrawal threshold to mechanical stimulation of the hind paw. The mechanical paw withdrawal threshold was recorded in duplicate and averaged for each paw, respectively. The mechanical paw withdrawal thresholds were measured at baseline (i.e., before CFA injection), 48 h after CFA injection, and at 10, 30, 60, and 120 min after pharmacological manipulation.

General Behavioral Methods. Methods for in vivo testing were similar to those described in our previously published work. Approximately 48 h following unilateral intraplantar injection of CFA, mice were injected with vehicle, anandamide, methanandamide, or AMG315.

Statistical Analysis. Two-way mixed ANOVA was used to analyze the main effect of drug treatments, main effect of time course or pre/post injection, and the interaction between drug treatments and time. Bonferroni post hoc tests were performed for all pairwise comparisons. Graph Pad Prism version 7.04 (GraphPad Software, San Diego, CA) were used for all analyses and figure generation.

Supporting Information

The Supporting Information is available free of charge on the ACS Publications website at DOI: 10.1021/acs.jmedchem.8b00611.

Abbreviations Used

CB1	cannabinoid receptor 1
CB2	cannabinoid receptor 2
AEA	anandamide
2-AG	2-arachidonoylglycerol
eCBs	endocannabinoids
FAAH	fatty acid amide hydrolase
MGL	monoacylglycerol lipase
ABHD6	α/β-hydrolase domain containing 6
COX-2	cyclooxygenases-2
LOXs	lipooxygenases
CNS	central nervous system
SAR	structure–activity relationship
HEK293	human embryonic kidney cell line
NMR	nuclear magnetic resonance
HPLC	high-performance liquid chromatography
CFA	complete Freund's adjuvant.

References

1. Lu, H. C.; Mackie, K. An introduction to the endogenous cannabinoid system. *Biol. Psychiatry* **2016**, *79* (7), 516– 525, DOI: 10.1016/j.biopsych.2015.07.028

2. Jarai, Z.; Wagner, J. A.; Goparaju, S. K.; Wang, L.; Razdan, R. K.; Sugiura, T.; Zimmer, A. M.; Bonner, T. I.; Zimmer, A.; Kunos, G. Cardiovascular effects of 2-arachidonoyl glycerol in anesthetized mice. *Hypertension* **2000**, *35* (2), 679– 684, DOI: 10.1161/01.HYP.35.2.679

3. Rouzer, C. A.; Marnett, L. J. Mechanism of free radical oxygenation of polyunsaturated fatty acids by cyclooxygenases. *Chem. Rev.* **2003**, *103* (6), 2239– 2304, DOI: 10.1021/cr000068x

4. Urquhart, P.; Nicolaou, A.; Woodward, D. F. Endocannabinoids and their oxygenation by cyclo-oxygenases, lipoxygenases and other oxygenases. *Biochim. Biophys. Acta, Mol. Cell Biol. Lipids* **2015**, *1851* (4), 366– 376, DOI: 10.1016/j.bbalip.2014.12.015

5. Alhouayek, M.; Muccioli, G. G. COX-2-derived endocannabinoid metabolites as novel inflammatory mediators. *Trends Pharmacol. Sci.* **2014**, *35* (6), 284– 292, DOI: 10.1016/j.tips.2014.03.001

6. Papahatjis, D. P.; Nahmias, V. R.; Nikas, S. P.; Schimpgen, M.; Makriyannis, A. Design and synthesis of (13S)-methyl-substituted arachidonic acid analogues: templates for novel endocannabinoids. *Chem. - Eur. J.* **2010**, *16* (13), 4091– 4099, DOI: 10.1002/chem.200902880

7. Hua, T.; Vemuri, K.; Nikas, S. P.; Laprairie, R. B.; Wu, Y.; Qu, L.; Pu, M.; Korde, A.; Jiang, S.; Ho, J. H.; Han, G. W.; Ding, K.; Li, X.; Liu, H.; Hanson, M. A.; Zhao, S.; Bohn, L. M.; Makriyannis, A.; Stevens, R. C.; Liu, Z. J. Crystal structures of agonist-bound human cannabinoid receptor CB1. *Nature* **2017**, *547* (7664), 468– 471, DOI: 10.1038/nature23272

8. Padgett, L. W.; Howlett, A. C.; Shim, J. Y. Binding mode prediction of conformationally restricted anandamide analogs within the CB1 receptor. *J. Mol. Signaling* **2014**, *3*, 5, DOI: 10.1186/1750-2187-3-5

9. Reggio, P. H. Endocannabinoid structure-activity relationships for interaction at the cannabinoid receptors. *Prostaglandins, Leukotrienes Essent. Fatty Acids* **2002**, *66* (2– 3), 143– 160, DOI: 10.1054/plef.2001.0343

10. Tian, X.; Guo, J.; Yao, F.; Yang, D. P.; Makriyannis, A. The conformation, location, and dynamic properties of the endocannabinoid ligand anandamide in a membrane bilayer. *J. Biol. Chem.* **2005**, *280* (33), 29788– 29795, DOI: 10.1074/jbc.M502925200

11. van der Stelt, M.; van Kuik, J. A.; Bari, M.; van Zadelhoff, G.; Leeflang, B. R.; Veldink, G. A.; Finazzi-Agro, A.; Vliegenthart, J. F.; Maccarrone, M. Oxygenated metabolites of anandamide and 2-arachidonoylglycerol: conformational analysis and interaction with cannabinoid receptors, membrane transporter, and fatty acid amide hydrolase. *J. Med. Chem.* **2002**, *45* (17), 3709– 3720, DOI: 10.1021/jm020818q

12. Abadji, V.; Lin, S.; Taha, G.; Griffin, G.; Stevenson, L. A.; Pertwee, R. G.; Makriyannis, A. (*R*)-Methanandamide, a chiral novel anandamide possessing higher potency and metabolic stability. *J. Med. Chem.* **1994**, *37* (12), 1889– 1893, DOI: 10.1021/jm00038a020

13. Bourne, C.; Roy, S.; Wiley, J. L.; Martin, B. R.; Thomas, B. F.; Mahadevan, A.; Razdan, R. K. Novel, potent THC/anandamide (hybrid) analogs. *Bioorg. Med. Chem.* **2007**, *15* (24), 7850– 7864, DOI: 10.1016/j.bmc.2007.08.039

14. Brizzi, A.; Brizzi, V.; Cascio, M. G.; Corelli, F.; Guida, F.; Ligresti, A.; Maione, S.; Martinelli, A.; Pasquini, S.; Tuccinardi, T.; Di Marzo, V. New resorcinol-anandamide ″hybrids″ as potent cannabinoid receptor ligands endowed with antinociceptive activity in vivo. *J. Med. Chem.* **2009**, *52* (8), 2506– 2514, DOI: 10.1021/jm8016255

15. Thakur, G. A.; Nikas, S. P.; Li, C.; Makriyannis, A. Structural requirements for cannabinoid receptor probes. *Handb. Exp. Pharmacol.* **2005**, *168* (168), 209– 246, DOI: 10.1007/3-540-26573-2_7

16. Yao, F.; Li, C.; Vadivel, S. K.; Bowman, A. L.; Makriyannis, A. Development of novel tail-modified anandamide analogs. *Bioorg. Med. Chem. Lett.* **2008**, *18* (22), 5912– 5915, DOI: 10.1016/j.bmcl.2008.07.110

17. Shelnut, E. L.; Nikas, S. P.; Finnegan, D. F.; Chiang, N.; Serhan, C. N.; Makriyannis, A. Design and synthesis of novel prostaglandin E2 ethanolamide and glycerol ester probes for the putative prostamide receptor(s). *Tetrahedron Lett.* **2015**, *56* (11), 1411– 1415, DOI: 10.1016/j.tetlet.2015.01.164

18. Hua, T.; Vemuri, K.; Pu, M.; Qu, L.; Han, G. W.; Wu, Y.; Zhao, S.; Shui, W.; Li, S.; Korde, A.; Laprairie, R. B.; Stahl, E. L.; Ho, J. H.; Zvonok, N.; Zhou, H.; Kufareva, I.; Wu, B.; Zhao, Q.; Hanson, M. A.; Bohn, L. M.; Makriyannis, A.; Stevens, R. C.; Liu, Z. J. Crystal structure of the human cannabinoid receptor CB1. *Cell* **2016**, *167* (3), 750– 762, DOI: 10.1016/j.cell.2016.10.004

19. Janero, D. R.; Korde, A.; Makriyannis, A. Ligand-assisted protein structure (LAPS): An experimental paradigm for characterizing cannabinoid-receptor ligand-binding domains. *Methods Enzymol.* **2017**, *593*, 217– 235, DOI: 10.1016/bs.mie.2017.06.022

20. Janero, D. R.; Yaddanapudi, S.; Zvonok, N.; Subramanian, K. V.; Shukla, V. G.; Stahl, E.; Zhou, L.; Hurst, D.; Wager-Miller, J.; Bohn, L. M.; Reggio, P. H.; Mackie, K.; Makriyannis, A. Molecular-interaction and signaling profiles of AM3677, a novel covalent agonist selective for the cannabinoid 1 receptor. *ACS Chem. Neurosci.* **2015**, *6* (8), 1400– 1410, DOI: 10.1021/acschemneuro.5b00090

21. Khanolkar, A. D.; Abadji, V.; Lin, S.; Hill, W. A.; Taha, G.; Abouzid, K.; Meng, Z.; Fan, P.; Makriyannis, A. Head group analogs of arachidonylethanolamide, the endogenous cannabinoid ligand. *J. Med. Chem.* **1996**, *39* (22), 4515– 4519, DOI: 10.1021/jm960152y

22. Nikas, S. P.; D'Souza, M.; Makriyannis, A. Enantioselective synthesis of (10S)- and (10R)-methyl-anandamides. *Tetrahedron* **2012**, *68* (31), 6329– 6337, DOI: 10.1016/j.tet.2012.05.010

23. Finnegan, D. F.; Shelnut, E. L.; Nikas, S. P.; Chiang, N.; Serhan, C. N.; Makriyannis, A. Novel tail and head group prostamide probes. *Bioorg. Med. Chem. Lett.* **2015**, *25* (6), 1228– 1231, DOI: 10.1016/j.bmcl.2015.01.064

24. Goutopoulos, A.; Fan, P.; Khanolkar, A. D.; Xie, X. Q.; Lin, S.; Makriyannis, A. Stereochemical selectivity of methanandamides for the CB1 and CB2 cannabinoid receptors and their metabolic stability. *Bioorg. Med. Chem.* **2001**, *9* (7), 1673– 1684, DOI: 10.1016/S0968-0896(01)00088-8

25. Lang, W.; Qin, C.; Lin, S.; Khanolkar, A. D.; Goutopoulos, A.; Fan, P.; Abouzid, K.; Meng, Z.; Biegel, D.; Makriyannis, A. Substrate specificity and stereoselectivity of rat brain microsomal anandamide amidohydrolase. *J. Med. Chem.* **1999**, *42* (5), 896– 902, DOI: 10.1021/jm980461j

26. Nikas, S. P.; Sharma, R.; Paronis, C. A.; Kulkarni, S.; Thakur, G. A.; Hurst, D.; Wood, J. T.; Gifford, R. S.; Rajarshi, G.; Liu, Y.; Raghav, J. G.; Guo, J. J.; Jarbe, T. U.; Reggio, P. H.; Bergman, J.; Makriyannis, A. Probing the carboxyester side chain in controlled

deactivation (−)-delta(8)-tetrahydrocannabinols. *J. Med. Chem.* **2015**, *58* (2), 665– 681, DOI: 10.1021/jm501165d

27. Kulkarni, S.; Nikas, S. P.; Sharma, R.; Jiang, S.; Paronis, C. A.; Leonard, M. Z.; Zhang, B.; Honrao, C.; Mallipeddi, S.; Raghav, J. G.; Benchama, O.; Jarbe, T. U. C.; Bergman, J.; Makriyannis, A. Novel C-ring-hydroxy-substituted controlled deactivation cannabinergic analogues. *J. Med. Chem.* **2016**, *59* (14), 6903– 6919, DOI: 10.1021/acs.jmedchem.6b00717

28. Nikas, S. P.; Alapafuja, S. O.; Papanastasiou, I.; Paronis, C. A.; Shukla, V. G.; Papahatjis, D. P.; Bowman, A. L.; Halikhedkar, A.; Han, X.; Makriyannis, A. Novel 1',1'-chain substituted hexahydrocannabinols: 9beta-hydroxy-3-(1-hexyl-cyclobut-1-yl)-hexahydrocannabinol (AM2389) a highly potent cannabinoid receptor 1 (CB1) agonist. *J. Med. Chem.* **2010**, *53* (19), 6996– 7010, DOI: 10.1021/jm100641g

29. Li, C.; Xu, W.; Vadivel, S. K.; Fan, P.; Makriyannis, A. High affinity electrophilic and photoactivatable covalent endocannabinoid probes for the CB1 receptor. *J. Med. Chem.* **2005**, *48* (20), 6423– 6429, DOI: 10.1021/jm050272i

30. Ogawa, G.; Tius, M. A.; Zhou, H.; Nikas, S. P.; Halikhedkar, A.; Mallipeddi, S.; Makriyannis, A. 3′-Functionalized adamantyl cannabinoid receptor probes. *J. Med. Chem.* **2015**, *58* (7), 3104– 3116, DOI: 10.1021/jm501960u

31. Kudalkar, S. N.; Nikas, S. P.; Kingsley, P. J.; Xu, S.; Galligan, J. J.; Rouzer, C. A.; Banerjee, S.; Ji, L.; Eno, M. R.; Makriyannis, A.; Marnett, L. J. 13-Methylarachidonic acid is a positive allosteric modulator of endocannabinoid oxygenation by cyclooxygenase. *J. Biol. Chem.* **2015**, *290* (12), 7897– 7909, DOI: 10.1074/jbc.M114.634014

32. Li, A. L.; Carey, L. M.; Mackie, K.; Hohmann, A. G. Cannabinoid CB2 agonist GW405833 suppresses inflammatory and neuropathic pain through a CB1 mechanism that is independent of CB2 receptors in mice. *J. Pharmacol. Exp. Ther.* **2017**, *362* (2), 296– 305, DOI: 10.1124/jpet.117.241901

33. Cheng, Y.; Prusoff, W. H. Relationship between the inhibition constant (Ki) and the concentration of inhibitor which causes 50% inhibition (I50) of an enzymatic reaction. *Biochem. Pharmacol.* **1973**, *22*, 3099– 3108, DOI: 10.1016/0006-2952(73)90196-2

34. Sharma, R.; Nikas, S. P.; Paronis, C. A.; Wood, J. T.; Halikhedkar, A.; Guo, J. J.; Thakur, G. A.; Kulkarni, S.; Benchama, O.; Raghav, J. G.; Gifford, R. S.; Jarbe, T. U.; Bergman, J.; Makriyannis, A. Controlled-deactivation cannabinergic ligands. *J. Med. Chem.* **2013**, *56* (24), 10142– 10157, DOI: 10.1021/jm4016075

35. Alapafuja, S. O.; Nikas, S. P.; Bharathan, I. T.; Shukla, V. G.; Nasr, M. L.; Bowman, A. L.; Zvonok, N.; Li, J.; Shi, X.; Engen, J. R.; Makriyannis, A. Sulfonyl fluoride inhibitors of fatty acid amide hydrolase. *J. Med. Chem.* **2012**, *55* (22), 10074– 10089, DOI: 10.1021/jm301205j

36. Patricelli, M. P.; Lashuel, H. A.; Giang, D. K.; Kelly, J. W.; Cravatt, B. F. Comparative characterization of a wild type and transmembrane domain-deleted fatty acid amide hydrolase: identification of the transmembrane domain as a site for oligomerization. *Biochemistry* **1998**, *37* (43), 15177– 15187, DOI: 10.1021/bi981733n

37. Lang, W.; Qin, C.; Hill, W. A.; Lin, S.; Khanolkar, A. D.; Makriyannis, A. High-performance liquid chromatographic determination of anandamide amidase activity in rat brain microsomes. *Anal. Biochem.* **1996**, *238* (1), 40– 45, DOI: 10.1006/abio.1996.0247

38. Qin, C.; Lin, S.; Lang, W.; Goutopoulos, A.; Pavlopoulos, S.; Mauri, F.; Makriyannis, A. Determination of anandamide amidase activity using ultraviolet-active amine derivatives and reverse-phase high-performance liquid chromatography. *Anal. Biochem.* **1998**, *261* (1), 8– 15, DOI: 10.1006/abio.1998.2713

39. Williams, J.; Wood, J.; Pandarinathan, L.; Karanian, D. A.; Bahr, B. A.; Vouros, P.; Makriyannis, A. Quantitative method for the profiling of the endocannabinoid metabolome by LC-atmospheric pressure chemical ionization-MS. *Anal. Chem.* **2007**, *79* (15), 5582– 5593, DOI: 10.1021/ac0624086

40. Zvonok, N.; Williams, J.; Johnston, M.; Pandarinathan, L.; Janero, D. R.; Li, J.; Krishnan, S. C.; Makriyannis, A. Full mass spectrometric characterization of human monoacylglycerol lipase generated by large-scale expression and single-step purification. *J. Proteome Res.* **2008**, *7* (5), 2158– 2164, DOI: 10.1021/pr700839z

41. Xu, S.; Hermanson, D. J.; Banerjee, S.; Ghebreselasie, K.; Clayton, G. M.; Garavito, R. M.; Marnett, L. J. Oxicams bind in a novel mode to the cyclooxygenase active site via a two-water-mediated H-bonding Network. *J. Biol. Chem.* **2014**, *289* (10), 6799– 6808, DOI: 10.1074/jbc.M113.517987

42. Guarnieri, F.; Weinstein, H. Conformational memories and the exploration of biologically relevant peptide conformations: An illustration for the gonadotropin-releasing hormone. *J. Am. Chem. Soc.* **1996**, *118* (24), 5580– 5589, DOI: 10.1021/ja952745o

43. Whitnell, R. M.; Hurst, D. P.; Reggio, P. H.; Guarnieri, F. Conformational memories with variable bond angles: Uses in conformational analysis in homogeneous and heterogeneous environments. *Biophys. J.* **2007**, 566a– 567a

44. Wilson, S. R.; Guarnieri, F. Calculation of rotational states of flexible molecules using simulated annealing. *Tetrahedron Lett.* **1991**, *32* (30), 3601– 3604, DOI: 10.1016/S0040-4039(00)79785-1

45. Ballesteros, J.; Weinstein, H. Integrated Methods for the Construction of Three-Dimensional Models and Computational Probing of Structure-Function Relations in G Protein-Coupled Receptors. In *Methods in Neurosciences*; Stuart, C. S., Ed.; Academic Press: San Diego, **1995**; Vol. 25, pp 366– 428.